Int. J. Production Economics 255 (2023) 108711

Contents lists available at ScienceDirect

International Journal of Production Economics

journal homepage: www.elsevier.com/locate/ijpe

Deviations from commitments: Markov decision process formulations for the role of energy storage

Ece Cigdem Karakoyun [a], Harun Avci [b], Ayse Selin Kocaman [a,*], Emre Nadar [a]

[a] Department of Industrial Engineering, Bilkent University, 06800 Ankara, Turkey
[b] Department of Industrial Engineering and Management Sciences, Northwestern University, Evanston, IL 60208, USA

ARTICLE INFO

Keywords:
Renewable energy
Storage
Electricity markets
Imbalance pricing
Negative electricity prices
Markov decision processes

ABSTRACT

We study the energy commitment, generation, and storage problem for a wind power producer who can own and operate a battery for different purposes. We consider two main problem settings: In the first setting, the producer may choose to deviate from her commitments based on the latest available information, using the battery to support such deviations. In the second setting, the producer is required to fulfill her commitments, using the battery as a back-up source. We also consider the special cases of these settings with no battery. In these settings, the producer decides how much energy to commit to purchasing or selling, how much energy to generate in the wind power plant, and how much energy to charge into or discharge from the battery. We formulate the producer's decision-making process as a Markov decision process (MDP) by taking into account uncertainties in the electricity price and wind speed in a market setting where the price can be negative. We analytically compare the total profits of the two main settings. We then conduct data-calibrated numerical experiments to examine the effects of system components, imbalance pricing parameters, negative prices, and wind availability on the system operations and profits. Using the battery to intentionally deviate from commitments rather than to minimize such deviations improves the total profit by 16.5%, while this change in the role of the battery increases the total imbalance by 16 times, on average, in our experiments.

1. Introduction

Over the last few decades, renewable energy sources such as wind and solar have received much attention in the development of power systems (Mathiesen et al. 2011, Pina et al. 2013, Weitemeyer et al. 2015). Many countries have set ambitious target levels for renewable energy generation (Laslett et al. 2017, Peker et al. 2018, Zhong et al. 2021). For example, with the ultimate goal of complete independence from fossil fuels by 2050, Denmark produced almost 40% of its electricity from wind power plants in 2018 (U.S. Department of Energy, 2018). Thanks to such initiatives in various countries, renewable energy sources are expected to meet 60% of the world's total energy requirement by 2050 (International Renewable Energy Agency, 2018).

Wind and solar power producers have been supported by governmental incentives for many years (Zhang et al. 2018, Liu et al. 2019). However, as the penetration of these sources increases in the power generation, these incentives are scheduled to expire or have already expired in many countries (Morales et al., 2013). Therefore, they start to become players in electricity markets to improve their profits (Wang et al., 2015). The renewable power producers participating in the electricity markets are in general subject to some penalties in case there is a mismatch between their energy commitment levels and the actual amounts they provide. Since renewable energy sources are uncertain and intermittent, extreme caution must be paid when the renewable power producers make advance commitment decisions in the presence of such penalties.

Co-locating renewable power generators with energy storage units, particularly batteries, has received much attention in recent years. The batteries can be used as a back-up source that serves as a hedge against the cost of imbalance due to fluctuating renewable outputs. They can also help respond effectively to price changes in the electricity markets. The producer can purchase energy from the market when the electricity price is low (or sometimes even negative[1]) and can sell the stored

* Corresponding author.
E-mail addresses: ece.cigdem@bilkent.edu.tr (E.C. Karakoyun), harun.avci@u.northwestern.edu (H. Avci), selin.kocaman@bilkent.edu.tr (A.S. Kocaman), emre.nadar@bilkent.edu.tr (E. Nadar).

[1] Negative electricity prices were observed in the markets run by the New York Independent System Operator (NYISO), Electric Reliability Council of Texas (ERCOT), California Independent System Operator (CAISO), and the European Energy Exchange (Zhou et al., 2019). For example, the proportion of negative-priced hours in the zones of CAISO has grown from 1.7%–2.3% to 6.3%–8.3% over the period 2013/14-2016/17 (Bajwa and Cavicchi, 2017).

https://doi.org/10.1016/j.ijpe.2022.108711
Received 3 January 2022; Received in revised form 30 September 2022; Accepted 1 November 2022
Available online 11 November 2022

energy to the market when the electricity price is high. Consequently, the number of renewable generation sites co-located with batteries has grown in the US from 19 paired sites in 2016 to 53 paired sites in 2019 (EIA, 2020). This trend will likely continue with further improvements in the battery storage technologies and investment costs (IRENA, 2021). Two recent examples are the Gemini solar project in Nevada and the Goyder South project in South Australia. Gemini is expected to contribute more than 1 GW of combined solar and battery energy capacities (EIA, 2020), while Goyder South has received development approval for 1.2 GW of wind energy, 0.6 GW of solar energy, and 0.9 GW of battery energy capacities (NEOEN, 2022).

Motivated by the increasing trend of renewable power generators co-located with batteries, we study the operations of a wind power plant paired with a battery. This energy system is connected via a transmission line to a spot market that operates with hourly commitments and settlements. We focus on detailed representations of the battery (e.g., energy and power capacities as well as asymmetric and imperfect efficiencies for storing/generating energy) and the transmission line (e.g., selling/purchasing capacity and imperfect efficiency). To examine various roles of the batteries, we consider two possible problem settings. In the first setting, the producer may intentionally deviate from her commitments for a better profit. In the second setting, however, the producer needs to fulfill her commitments as much as possible, storing any excess wind energy as long as the battery capacity allows. We also consider two other settings that are the special cases of the above settings with no battery. In these settings, the producer decides how much energy to commit in the market, to generate in the wind power plant, and to charge into or discharge from the battery. Since the transmission line has a finite capacity and negative electricity prices may occur in our model, the producer also decides how much energy to curtail in the wind power plant.

The intentional deviations are observed in both US-type and European-type electricity markets. The regulations of the California Independent System Operator (CAISO) imply that the producers may intentionally engage in uninstructed deviations from generation schedules by strategically bidding at high prices or withholding their energy capacity (CAISO 1998, 2013). This situation may also arise in the other markets under the control of the New York Independent System Operator (NYISO), Midcontinent Independent System Operator (MISO), and ISO New England (CAISO, 2007). Examples for the European-type markets include those in the Netherlands and Belgium (Röben and De Haan 2019, Eicke et al. 2021). To exemplify how the intentional deviations can be financially attractive for a wind power producer, we consider the following two cases: If the generated wind energy falls short of the committed amount, the producer is expected to compensate for the shortage from the battery and pay a penalty for the remainder (if there is any). If the generated wind energy exceeds the committed amount, the producer is expected to store or curtail the excess amount. However, when the electricity price and wind speed that are uncertain at the time of commitment decision become known as time progresses, the opportunity cost of discharging or charging the battery to meet the commitment may be higher than the cost of (i.e., the corresponding penalty for) not meeting the commitment. Therefore, the producer may prefer to stay in imbalance, motivating us to study the first problem setting.

While the intentional deviations can be financially attractive for the producers, they may lower the reliability of the grid operations. Therefore, some countries explicitly implement strict regulations to prevent this practice. For example, the intentional deviations were allowed in the German electricity market from 2003 to 2009, but these deviations gradually disappeared after 2011 when this practice was forbidden by the German system operator (Eicke et al. 2021, Finnah and Gönsch 2021, Finnah et al. 2022). Strategically causing an energy imbalance is also forbidden in Italy (Lisi and Edoli, 2018). Under such regulations, the producers must fulfill their commitments as much as possible even when it is financially unattractive to do so, motivating us to study the second problem setting.

We formulate the real-time decision-making process of the wind power producer as an MDP. The intentional deviations in our study can arise due to the price and wind uncertainties that are resolved over time. (The intentional deviations could also arise due to the price differences between sequential markets. This possibility is beyond the scope of this study as we focus on a single market structure.) Therefore, investigating the different roles of the battery (i.e., a strategic tool to intentionally deviate from commitments in the first setting or a back-up source to fulfill commitments in the second setting) becomes critical in the presence of price and wind uncertainties. The two settings would be identical if there were no such uncertainties (under a mild condition in the initial period of our MDP). Our MDP framework enables us to effectively capture these uncertainties in the hour-ahead market structure by allowing future uncertainties to be resolved only when the producer moves forward in time. The producer can thus make adaptive decisions based on the realizations of uncertainties in real-time. In addition, MDPs provide clean analytical formulations by capturing the complex dynamics inherent in many real-life problems like ours. Focusing on the hour-ahead market structure with our MDP framework, we are able to analytically compare the total profits of the two settings and numerically solve the realistic-size problem instances to optimality.

We conduct an extensive numerical study by focusing on the historical electricity price and wind speed data from a market where negative prices were observed in the past. We construct time series models that can represent the historical data with acceptable accuracy levels. Our time series models capture the mean-reversion, seasonality, and spike components of electricity prices, as well as the significant seasonal patterns of wind speeds. We incorporate these models into our MDP with the help of exogenous state variables. We then solve the problem with a backward dynamic programming algorithm for various realistic configurations of our energy system.

We contribute to the energy literature as follows: We present MDP formulations for the energy commitment, generation, and storage problem of a producer who uses the battery (i) as a strategic tool for supporting intentional deviations from her commitments or (ii) as a back-up source for fulfilling her commitments. We analytically show that the role of the battery in (i) brings an additional profit to the producer, while this role of the battery is likely to be undesirable for the market. We numerically investigate the impacts of the system components, imbalance pricing parameters, negative electricity prices, and wind availability in these settings when the battery is available and when it is not. We summarize below the key findings from our numerical study that may have policy implications for both regulatory authorities and wind power producers in electricity markets:

- If the producer cannot make intentional deviations, the existence of a battery reduces the energy imbalance. However, if she is allowed to make intentional deviations, the existence of a battery has an opposite effect, inducing the negative imbalance more than the positive imbalance.
- When the intentional deviations are allowed, the imbalance amounts can be reduced by properly choosing the imbalance pricing parameters. However, the imbalance amounts in the absence of a battery are not affected by the symmetric imbalance pricing parameters.
- When the intentional deviations are not allowed, the imbalance pricing parameters substantially affect the imbalance amounts of the producer with no battery. However, the existence of a battery makes the producer relatively insensitive to the imbalance pricing parameters.
- When the intentional deviations are not allowed, a higher battery capacity tends to induce a lower imbalance amount. When the intentional deviations are allowed, a higher battery capacity may

induce a lower imbalance amount under a low transmission line capacity, whereas it induces a higher imbalance amount under a high transmission line capacity.
- Although the existence of a battery provides the opportunity to purchase energy when the electricity prices are negative, the total profits in all settings suffer from an increment in the negative price occurrence frequency. The supporting role of the battery for intentional deviations becomes more valuable as this frequency grows.

The remainder of this paper is organized as follows: Section 2 reviews the related literature. Section 3 formulates the energy commitment, generation, and storage problem for each of the two settings. Section 4 presents our time series models for the electricity price and wind speed as well as their discrete-state representations that we require for our numerical experiments. Section 5 presents our numerical results and Section 6 concludes.

2. Related literature

There is a vast amount of literature on the joint optimization of renewable power generation and energy storage in electricity markets. Most studies have focused on stochastic optimization models (e.g., Garcia-Gonzalez et al. 2008, Ding et al. 2014, Castronuovo et al. 2014, Ding et al. 2015, Nasrolahpour et al. 2016, Al-Swaiti et al. 2017, Gomes et al. 2017, 2019, Khazali et al. 2021, Xu et al. 2020, Terça and Wozabal 2020, Khosravi et al. 2022, Dadashi et al. 2022). We refer the reader to Parker et al. (2019) and Elshurafa (2020) for comprehensive reviews of this literature. We restrict our literature review to more closely related papers that study MDP representations of the problem.

Löhndorf and Minner (2010) study the bidding strategy of a renewable power producer with storage option in a day-ahead electricity market. Hannah and Dunson (2011) apply an approximate dynamic programming approach to the day-ahead commitment problem of a wind power producer with a storage unit. Löhndorf et al. (2013) examine the energy commitment and storage decisions of a hydroelectric storage operator in day-ahead and intraday electricity markets. Kim and Powell (2011) derive the optimal commitment amount that should be submitted by a wind power producer with storage option in a real-time market with hour-ahead adjustments. Gönsch and Hassler (2016) present an approximate policy iteration algorithm for the commitment problem of a wind power producer with a storage unit. Hassler (2017) develops heuristic decision rules for the short-term trading of renewable energy for a producer with storage option. Díaz et al. (2019) focus on the participation of a wind power producer with a storage unit in multi-stage electricity markets. Finally, Finnah and Gönsch (2021) construct an approximate dynamic programming algorithm for the commitment problem of a wind power producer integrated with a battery and a hydrogen based storage unit.

The above studies do not examine the potential supporting role of the storage unit to intentionally deviate from commitments. Specifically, in these studies, the renewable power producer can utilize the storage unit only to reduce the energy imbalance as much as possible. Therefore, there are no generation/storage decisions in their MDP formulations. In addition, none of these studies investigate the effect of negative electricity prices. However, as the renewable power generation grows in electricity markets, the negative prices are unavoidably observed more frequently, increasing the need for this investigation (De Jonghe et al. 2011, Vilim and Botterud 2014, Ederer 2015). These studies, except Finnah and Gönsch (2021), also assume that electricity can only be transmitted from the energy system to the market (i.e., the renewable power producer can only sell energy to the market). However, when the electricity price is too low or negative, the producer with a storage unit may want to benefit from these prices by purchasing energy from the market. Lastly, in Hannah and Dunson (2011), Kim and Powell (2011), and Gönsch and Hassler (2016), the imbalance price applies only to the case of negative imbalance (i.e., when the committed amount exceeds the actual amount provided). Löhndorf et al. (2013) assume that when the producer cannot fulfill her commitment in the day-ahead market, the imbalance can be cleared in the intraday market. Therefore, they do not explicitly model the penalty costs that can be observed in real-time. Hassler (2017) and Finnah and Gönsch (2021) assume that the imbalance prices are the same regardless of the direction of imbalance (negative or positive). We relax all of the above assumptions in this study.

To our knowledge, our study is the first attempt to develop an MDP framework to distinguish between the following two roles of a battery: when it is used to support either intentional deviations from commitments or fulfillment of commitments. We present and compare two different MDP formulations for these different roles of the battery under uncertainty. We investigate the effects of system components (battery and transmission line) and spot market characteristics (negative electricity prices, two-way system-market transactions, and asymmetric imbalance prices) on the system operations and profits in different environments.

3. Problem formulation

We consider an energy system that consists of a wind power plant and a battery. See Fig. 1 for an illustration of this system. The producer can generate energy from the wind power plant and the battery. The producer can also store energy by charging the battery. The producer participates in a single spot market that involves hour-ahead commitments and hourly settlements. The single-market assumption has been made in many papers that focus on the operations of renewable power producers in electricity markets; see, for example, Löhndorf and Minner (2010), Kim and Powell (2011), Jiang and Powell (2015), Gönsch and Hassler (2016), Hassler (2017), Sunar and Birge (2019), and Finnah and Gönsch (2021). Considering the uncertainties in electricity price and wind speed, the producer should make several challenging decisions in each time period: how much energy to generate in the wind power plant, to charge/discharge into/from the battery, and to commit to selling/purchasing to/from the market in the next period. The system makes only a very limited contribution to the overall energy supply in the market; therefore, the producer can be viewed as a price-taker. This assumption has also been made in many papers that focus on the operations of renewable power producers in electricity markets; see, for example, Pinson et al. (2007), Löhndorf and Minner (2010), Kim and Powell (2011), Ding et al. (2015), Gönsch and Hassler (2016), Hassler (2017), and Díaz et al. (2019).

The battery has finite energy and power capacities. The energy capacity of the battery is the maximum amount of energy that can be stored in the battery. The power capacity is the maximum amount of energy that can be generated (by discharging the battery) or stored (by charging the battery) in a single time period. We denote the energy capacity of the battery by C_S. We denote the generation and storage capacities by K_D and K_C, respectively, in power units. The transmission line also has a finite power capacity. We denote this capacity by K_T in power units. For notational convenience, we define $C_C = K_C\Delta t$, $C_D = K_D\Delta t$, and $C_T = K_T\Delta t$, where Δt is the length of one time period. For the battery, we denote by $\gamma \in (0,1]$ and $\theta \in (0,1]$ the efficiency parameters in the discharging and charging modes, respectively. For the transmission line, we denote by $\tau \in (0,1]$ the efficiency parameter in both the selling and purchasing modes. These parameters represent the ratio of energy output to energy input.

We study the energy commitment, generation, and storage problem in this system via a dynamic model over a finite planning horizon of T periods. Let $\mathcal{T} := \{1,2,\dots,T\}$ denote the set of periods. We define $S_t \in [0, C_S]$ as the amount of energy accumulated in the battery at the beginning of period t. The producer can either sell or purchase energy in any particular period. We define $Q_t \in \mathbb{R}$ as the amount of energy that the producer is obligated to sell if $Q_t \geq 0$ and to purchase

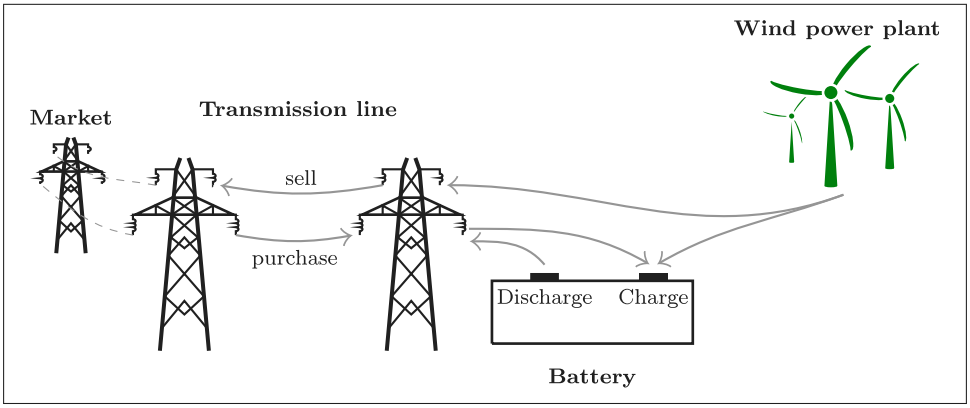

Fig. 1. Illustration of the energy system.

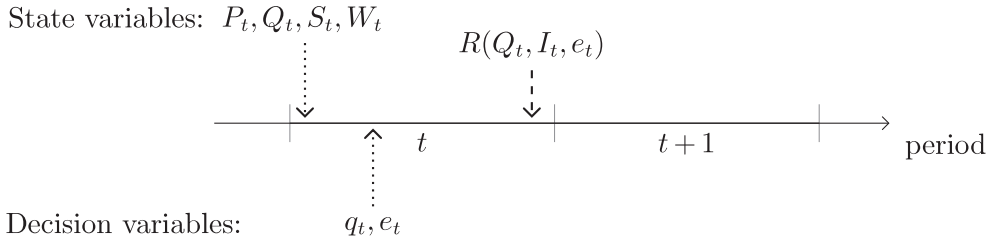

Fig. 2. Sequence of events in each period.

if $Q_t < 0$ in period t, in order to fulfill the commitment that she has made in period $t-1$. We include S_t and Q_t in our state description. We define $W_t \in \mathbb{R}_+$ as the wind speed in period t and $f(W_t)$ as the maximum amount of wind energy that can be generated in period t. We derive $f(W_t)$ from the multiplication of the power output of a wind turbine when the wind speed is W_t, the number of turbines in the wind power plant, and the period length Δt. Lastly, we define $P_t \in \mathbb{R}$ as the electricity price in period t. We also include the tuple $I_t := (P_\kappa, W_\kappa)_{\kappa \le t}$ in our state description. The state tuple I_t evolves over time according to an exogenous stochastic process.

In any period $t \in \mathcal{T}$, the producer first observes the exogenous state variables (P_t and W_t) as well as the endogenous state variables (Q_t and S_t). The producer then determines the amount of energy to be committed to selling or purchasing in period $t+1$ by signing the contract in period t, which we denote by $q_t \in \mathbb{R}$, and the actual amount of energy to be sold or purchased in period t, which we denote by $e_t \in \mathbb{R}$. The transmission line capacity implies that $e_t \le \tau C_T$ if $e_t \ge 0$ (the energy is sold) and $-C_T \le e_t$ if $e_t < 0$ (the energy is purchased). The market pays the purchasing cost for the amount of energy it actually receives, whereas the producer pays the purchasing cost for the amount of energy supplied on the other end of the transmission line. Although the maximum amount of energy that can be supplied to the transmission line (on either end) is C_T, the actual amount of energy received by the market (and thus sold by the producer) cannot exceed τC_T due to the efficiency loss during transmission. An alternative interpretation of such market transactions is that the producer is obligated to pay the grid usage fee per unit energy sold or purchased. Finally, we note that the actual amount of energy sold or purchased in period t may be different from the state variable Q_t. See Fig. 2 for an illustration of the sequence of events.

The producer faces the challenge of ensuring that the energy committed to selling/purchasing is sold/purchased in real-time. If the producer does not fulfill her contractual commitment in real-time (i.e., $Q_t \ne e_t$), she pays a penalty cost that varies with her deviation (i.e., the difference between the committed and realized amounts). There are two possible cases: (i) The commitment is less than the amount that the producer indeed provides in real-time (i.e., $Q_t < e_t$); the producer experiences a 'positive imbalance.' (ii) The commitment is greater than the amount that the producer indeed provides in real-time (i.e., $Q_t > e_t$); the producer experiences a 'negative imbalance.'

The imbalance pricing mechanisms may vary across electricity markets. For example, some European-type markets, such as the ones in Germany, the Netherlands, and Belgium, adopt a single pricing mechanism in which the imbalance price is often determined by the balancing (real-time) price and the same price is charged for both positive and negative imbalances (Brijs et al., 2019). Some other European-type markets, such as the ones in the Nordic countries (for generation units), France, and the UK, adopt a dual pricing mechanism in which the imbalance price depends on the outcome of sequential markets and the direction of imbalance (Chaves-Ávila et al., 2014). In the US-type markets, the imbalance price is based on the realized price of the market (van der Veen et al. 2012, PJM 2015, MISO 2022). Different system operators in the US-type markets may impose different imbalance pricing mechanisms. For example, NYISO penalizes only negative imbalances whereas CAISO and MISO penalize both positive and negative imbalances (Papavasiliou and Oren 2008, Kim and Powell 2011, Jiang and Powell 2015, MISO 2022).

In our study, we implement a market-based imbalance pricing mechanism that is mostly related to the US-type markets. Specifically, we take the imbalance prices as linear functions of the market price: the imbalance price in the case of positive imbalance is always $K_p^+(K_p^-)$ times the market price and the imbalance price in the case of negative imbalance is always $K_n^+(K_n^-)$ times the market price. This assumption is in line with the literature (e.g., Löhndorf and Minner 2010, Kim and Powell 2011, Jiang and Powell 2015, Gönsch and Hassler 2016, Hassler 2017, Finnah and Gönsch 2021, Finnah et al. 2022). To approach the problem in a more general sense, we ensure that the producer is settled with a penalized price in the cases of positive and negative imbalances. This principle has been adopted in many related papers (e.g., Pinson

et al. 2007, Löhndorf and Minner 2010, Boomsma et al. 2014). The payoff in period t is given by

$$R(Q_t, I_t, e_t) = \begin{cases} Q_t P_t + K_p^+ P_t(e_t - Q_t) & \text{if } P_t \geq 0 \text{ and } Q_t < e_t, \\ Q_t P_t - K_n^+ P_t(Q_t - e_t) & \text{if } P_t \geq 0 \text{ and } Q_t \geq e_t, \\ Q_t P_t + K_p^- P_t(e_t - Q_t) & \text{if } P_t < 0 \text{ and } Q_t < e_t, \\ Q_t P_t - K_n^- P_t(Q_t - e_t) & \text{if } P_t < 0 \text{ and } Q_t \geq e_t, \end{cases}$$

where $0 \leq K_p^+ < 1 < K_n^+$ and $0 \leq K_n^- < 1 < K_p^-$. In this formulation, $K_p^+ P_t$ and $K_n^+ P_t$ denote the imbalance prices when the electricity price is nonnegative in the cases of positive and negative imbalances, respectively. Likewise, $K_p^- P_t$ and $K_n^- P_t$ denote the imbalance prices when the electricity price is negative in the cases of positive and negative imbalances, respectively. The first term of the payoff function corresponds to the instant revenue $Q_t P_t$ in period t, which may be negative due to negative electricity prices or negative commitment levels. The second term of the payoff function captures the penalty payments in period t.

We consider two possible problem settings: In the first setting, the producer can intentionally deviate from her commitments in real-time transactions (Section 3.1). In the second setting, the producer should always fulfill her commitments as much as possible while keeping the curtailment at the minimum level (Section 3.2).

3.1. The use of battery for intentional deviation

In this setting, the producer may choose to deviate from her commitments in real-time transactions by jointly optimizing the available energy sources (wind power plant and battery). Specifically, she determines the amount of wind energy that will be generated in period t, which we denote by $w_t \in \mathbb{R}_+$, and the amount of energy that will be discharged or charged in period t, which we denote by $s_t \in \mathbb{R}$. The battery is discharged if $s_t \geq 0$ and charged if $s_t < 0$. Let $\mathbb{U}(Q_t, S_t, I_t)$ denote the set of action triplets (q_t, s_t, w_t) that are admissible in state (Q_t, S_t, I_t). For any action triplet $(q_t, s_t, w_t) \in \mathbb{U}(Q_t, S_t, I_t)$, the following conditions must hold: The observed wind speed limits the amount of wind energy that can be generated in the form of $0 \leq w_t \leq f(W_t)$. The energy and power capacities of the battery imply that $-\min\{C_S - S_t, C_C\} \leq s_t \leq \min\{S_t, C_D\}$. The amount of energy that can be charged/discharged into/from the battery and the amount of wind energy that can be generated are restricted together by the transmission line capacity (see Lew et al. 2013, Bird et al. 2016). Thus, the power capacity of the transmission line implies that $\gamma s_t + w_t \leq C_T$ if $s_t \geq 0$ and $-\tau C_T \leq s_t/\theta + w_t \leq C_T$ if $s_t < 0$. The state variables S_t and Q_t evolve over time as follows: $S_{t+1} = S_t - s_t$ and $Q_t = q_{t-1}$.

There are three different types of decisions that we need to consider in order to formulate the amount of energy sold or purchased in any period t: (i) A certain amount of energy is generated by discharging the battery ($s_t \geq 0$). The resulting energy together with the generated wind energy is sold in the market. (ii) A certain amount of energy is stored by charging the battery ($s_t < 0$). If the generated wind energy is sufficient to charge the battery ($s_t/\theta \geq -w_t$), the excess wind energy is sold to the market. (iii) If the generated wind energy is not sufficient to charge the battery ($s_t/\theta < -w_t$), the required additional energy is purchased from the market. Hence, the amount of energy sold or purchased in period t is defined as a function of actions s_t and w_t:

$$e_t = E(s_t, w_t) := \begin{cases} (\gamma s_t + w_t)\tau & \text{if } s_t \geq 0, \\ (s_t/\theta + w_t)\tau & \text{if } -w_t \leq s_t/\theta < 0, \\ (s_t/\theta + w_t)/\tau & \text{if } s_t/\theta < -w_t \leq 0. \end{cases}$$

Since the decision variable s_t is not constrained by the commitment level Q_t, the producer has the flexibility to use the battery as a strategic tool to intentionally deviate from her commitments. When the battery has sufficient energy to fulfill the commitment, the producer may choose to stay in negative imbalance in order to keep the battery full enough to benefit from high electricity prices in the future. The producer may also choose to stay in positive imbalance in order to keep the battery empty enough in anticipation of lower prices in the future.

Without loss of optimality, the amount of energy committed to selling (i.e., $q_t \geq 0$) can be restricted to take values no larger than the maximum amount of energy that can be sold (bounded by the transmission line capacity, i.e., $q_t \leq \tau C_T$). In addition, the amount of energy committed to purchasing (i.e., $q_t < 0$) can be restricted to take values no larger than the maximum amount of energy that can be stored (bounded by the available storage capacity $\frac{C_S - (S_t - s_t)}{\theta\tau}$, the charging capacity $\frac{C_C}{\theta\tau}$, and the transmission line capacity C_T). Therefore, at optimality, $-\min\left\{\frac{C_S-(S_t-s_t)}{\theta\tau}, \frac{C_C}{\theta\tau}, C_T\right\} \leq q_t \leq \tau C_T$, $\forall t \in \mathcal{T}$, and $-\min\left\{\frac{C_S-S_t}{\theta\tau}, \frac{C_C}{\theta\tau}, C_T\right\} \leq Q_t \leq \tau C_T$, $\forall t \in \mathcal{T}\backslash\{1\}$.

A control policy π is the sequence of decision rules $(\eta_t^\pi(Q_t^\pi, S_t^\pi, I_t))_{t\in\mathcal{T}}$, where $\eta_t^\pi(Q_t^\pi, S_t^\pi, I_t) := (q_t^\pi(Q_t^\pi, S_t^\pi, I_t), s_t^\pi(Q_t^\pi, S_t^\pi, I_t), w_t^\pi(Q_t^\pi, S_t^\pi, I_t))$, and Q_t^π and S_t^π denote the random state variables governed by policy π, $\forall t \in \mathcal{T}\backslash\{1\}$. We denote the set of all admissible control policies by Π. For any initial state (Q_1, S_1, I_1), the optimal expected total cash flow over the finite horizon is given by

$$\max_{\pi\in\Pi} \mathbb{E}\left[\sum_{t\in\mathcal{T}} R(Q_t^\pi, I_t, E(s_t^\pi(Q_t^\pi, S_t^\pi, I_t), w_t^\pi(Q_t^\pi, S_t^\pi, I_t)))\middle| Q_1, S_1, I_1\right].$$

For each period $t \in \mathcal{T}$ and each state (Q_t, S_t, I_t), the optimal profit function $v_t^*(Q_t, S_t, I_t)$ can be calculated with the following dynamic programming recursion:

$$v_t^*(Q_t, S_t, I_t) = \max_{(q_t, s_t, w_t)\in\mathbb{U}(Q_t, S_t, I_t)} \left\{ R(Q_t, I_t, E(s_t, w_t)) + \mathbb{E}_{I_{t+1}|I_t}\left[v_{t+1}^*(q_t, S_{t+1}, I_{t+1})\right]\right\} \tag{1}$$

where $v_T^*(Q_T, S_T, I_T) = 0$. Note that $v_1^*(Q_1, S_1, I_1)$ is the optimal expected total cash flow for the initial state (Q_1, S_1, I_1) over the finite horizon.

3.2. The use of battery for commitment fulfillment

In this setting, the producer is not allowed to intentionally deviate from her commitments in real-time transactions. The producer must utilize the available energy sources to fulfill her commitments as much as possible, storing any excess wind energy as long as the battery capacity allows. In other words, the amount of energy to be sold/purchased in period t should be as close to the state variable Q_t as possible with the minimum curtailment level. Therefore, we choose the actions s_t and w_t in this setting as follows:

$$\hat{s}_t = \begin{cases} \min\left\{S_t, C_D, (Q_t/\tau - f(W_t))/\gamma\right\} & \text{if } Q_t/\tau \geq f(W_t) \geq 0, \\ -\min\left\{C_S - S_t, C_C, (f(W_t) - Q_t/\tau)\theta\right\} & \text{if } f(W_t) > Q_t/\tau \geq 0, \\ -\min\left\{C_S - S_t, C_C, (f(W_t) - \tau Q_t)\theta\right\} & \text{if } f(W_t) \geq 0 > \tau Q_t, \end{cases}$$

and

$$\hat{w}_t = \begin{cases} f(W_t) & \text{if } Q_t/\tau \geq f(W_t) \geq 0, \\ Q_t/\tau + \min\left\{(C_S - S_t)/\theta, C_C/\theta, f(W_t) - Q_t/\tau\right\} & \text{if } f(W_t) > Q_t/\tau \geq 0, \\ \tau Q_t + \min\left\{(C_S - S_t)/\theta, C_C/\theta, f(W_t) - \tau Q_t\right\} & \text{if } f(W_t) \geq 0 > \tau Q_t. \end{cases}$$

Note that in this setting the producer determines only the commitment amount $q_t \in \mathbb{R}$.

The above formulation implies that the battery is charged only when the wind energy potential exceeds the commitment, and it is discharged only when the wind energy potential falls short of the commitment. More specifically, if the commitment exceeds the maximum amount of wind energy that can be generated, the required energy $(Q_t/\tau - f(W_t))$ is discharged from the battery with efficiency factor γ to meet the commitment. However, the amount of energy discharged is restricted by the storage level S_t and the discharging capacity C_D. If the producer committed to selling energy to the market and the maximum amount of wind energy that can be generated exceeds the commitment, the excess

energy ($f(W_t) - Q_t/\tau$) is charged into the battery with efficiency factor θ. If the producer committed to purchasing energy from the market, the maximum amount of wind energy that can be generated along with the energy purchased from the market ($f(W_t) - \tau Q_t$) is charged into the battery with efficiency factor θ. In both cases, the amount of energy charged must respect the battery's energy capacity C_S and charging capacity C_C; these capacity constraints induce curtailment of some wind energy if the wind energy potential is too high. Since the producer makes her commitment decisions in any period by taking into account the state of the battery in the next period, the amount of energy committed to purchasing from the market can indeed be purchased and stored in real-time at optimality.

The amount of energy sold/purchased in real-time can be formulated as a function of Q_t, S_t, and I_t:

$$\widehat{e}_t = E(Q_t, S_t, I_t) := \begin{cases} \left(\min\left\{\gamma S_t, \gamma C_D, Q_t/\tau - f(W_t)\right\} + f(W_t) \right) \tau & \text{if } Q_t/\tau \geq f(W_t) \geq 0, \\ Q_t & \text{if } f(W_t) > Q_t/\tau \geq 0, \\ Q_t & \text{if } f(W_t) \geq 0 > \tau Q_t. \end{cases}$$

If the maximum amount of wind energy that can be generated is greater than the commitment level, then $E(Q_t, S_t, I_t) = Q_t$. Therefore, the only possible direction of imbalance that the producer can experience is the negative imbalance in which the producer sells energy to the market in real-time less than her commitment. This scenario may arise due to the limited discharging capacity and the wind energy potential less than expected. The shortfall in this case is compensated at a penalized price.

Let $\widehat{\mathbb{U}}(Q_t, S_t, I_t)$ denote the set of actions q_t that are admissible in state (Q_t, S_t, I_t). Recall that, at optimality, $-\min\left\{\frac{C_S-(S_t-\widehat{s}_t)}{\theta\tau}, \frac{C_C}{\theta\tau}, C_T\right\} \leq q_t \leq \tau C_T$, $\forall t \in \mathcal{T}$, and $-\min\left\{\frac{C_S-S_t}{\theta\tau}, \frac{C_C}{\theta\tau}, C_T\right\} \leq Q_t \leq \tau C_T$, $\forall t \in \mathcal{T}\backslash\{1\}$. A control policy π is the sequence of decision rules $(q_t^\pi(Q_t^\pi, S_t^\pi, I_t))_{t\in\mathcal{T}}$, where Q_t^π and S_t^π denote the random state variables governed by policy π, $\forall t \in \mathcal{T}\backslash\{1\}$. We denote the set of all admissible control policies by $\widehat{\Pi}$. For any initial state (Q_1, S_1, I_1), the optimal expected total cash flow over the finite horizon is given by

$$\max_{\pi\in\widehat{\Pi}} \mathbb{E}\left[\sum_{t\in\mathcal{T}} R(Q_t^\pi, I_t, E(Q_t^\pi, S_t^\pi, I_t)) \middle| Q_1, S_1, I_1\right].$$

For each period $t \in \mathcal{T}$ and each state (Q_t, S_t, I_t), the optimal profit function $\widehat{v}_t^*(Q_t, S_t, I_t)$ can be calculated with the following dynamic programming recursion:

$$\widehat{v}_t^*(Q_t, S_t, I_t) = \max_{q_t\in\widehat{\mathbb{U}}(Q_t,S_t,I_t)} \left\{R(Q_t, I_t, E(Q_t, S_t, I_t)) + \mathbb{E}_{I_{t+1}|I_t}\left[\widehat{v}_{t+1}^*(q_t, S_{t+1}, I_{t+1})\right]\right\} \quad (2)$$

where $\widehat{v}_T^*(Q_T, S_T, I_T) = 0$. Note that $\widehat{v}_1^*(Q_1, S_1, I_1)$ is the optimal expected total cash flow for the initial state (Q_1, S_1, I_1) over the finite horizon.

The following proposition compares the total cash flows of the two problem settings above. The proof is available in the Appendix.

Proposition 1. $v_1^*(Q_1, S_1, I_1) \geq \widehat{v}_1^*(Q_1, S_1, I_1)$.

Proposition 1 implies that the option of deviating from the commitments brings an additional profit to the producer. In Section 5, we will numerically compare the total cash flows of the two problem settings with data-calibrated instances.

4. Experimental setup for the numerical study

As mentioned in the Introduction, the hour-ahead market structure allows for a computationally tractable MDP formulation that enables us to solve the realistic-size problem instances to optimality under uncertainty. This market structure can be arguably viewed as a real-time market structure in the US (Kim and Powell 2011, Jiang and Powell 2015). Also, recall that the intentional deviations in our study may be financially attractive thanks to the price and wind uncertainties that can only be resolved over time. Since the hour-ahead uncertainties can be thought of as less significant than the uncertainties over longer time frames, the day-ahead and intraday market structures would likely amplify the numerical insights derived in this study. In our numerical study, we use the real-time electricity prices obtained from NYISO, which is one of the largest and most liquid electricity markets where negative prices are observed (Zhou et al., 2019).

In this section, using the historical data available from the State of New York, we develop two distinct time series models for the electricity price and wind speed, respectively (Sections 4.1–4.2). We incorporate these parametric models into our MDP by utilizing the exogenous state variables. We then discretize the continuous space of the exogenous state variables for our numerical calculations (Section 4.3). We conduct numerical experiments for various configurations of our energy system in Section 5. We set the period length to be one hour in our experiments.

4.1. Time series model for the electricity price

We consider the real-time market electricity price data available for Albany, in the State of New York, between the years 2007 and 2019 in which the price is set every five minutes. Since the real-time transactions in Albany are regulated by the NYISO, we retrieve the price data from NYISO (2019). The average, median, minimum, and maximum values of the price are \$45.14, \$34.09, –\$3678.02, and \$3393.33, respectively. As we assume hourly periods, we include the price value of every hour of the day in our time series model. Our time series model consists of the components of seasonality (ψ_t'), mean reversion (ρ_t), and spike (j_t). We model the seasonality component via linear regression, the mean-reversion component via an autoregressive of order one process, and the spike component via an empirical distribution. The spike component of the price represents sudden and large moves in the price that are independent across periods.

We take the following steps to construct our time series model: We first deseasonalize the price data to eliminate the effect of seasonal variation on our spike identification. Following Zhou et al. (2019), we fit a linear regression to the price data to obtain a seasonality model $\{\hat{\psi}_t\}_{t\in\mathcal{T}}$:

$$\psi_t = \gamma_1^{(p)} + \sum_{i=1}^{11} \gamma_{2i}^{(p)} D_t^{2i} + \sum_{j=1}^{6} \gamma_{3j}^{(p)} D_t^{3j}$$

where $\gamma_1^{(p)}$ is a constant, and $\gamma_{2i}^{(p)}$ and $\gamma_{3j}^{(p)}$ are the coefficients of the dummy variables D_t^{2i} and D_t^{3j}, that are equal to one if period t is in month i and week day j, respectively. We calculate the deseasonalized prices $\{d_t\}_{t\in\mathcal{T}}$ by removing the seasonal effect from the observed prices $\{p_t\}_{t\in\mathcal{T}}$ (i.e., $d_t = p_t - \hat{\psi}_t$). We model the spikes $\{j_t\}_{t\in\mathcal{T}}$ as a compound Bernoulli process; a spike occurs with probability λ and its size follows an empirical distribution. In order to identify the spikes, we consider the highest five percent and the lowest five percent of the deseasonalized prices as outliers (see Janczura et al. 2013 for a detailed discussion on spike identification). The spikes $\{j_t\}_{t\in\mathcal{T}}$ are determined by the differences between these outliers and the mean of the remaining deseasonalized prices after these outliers are removed. We take $j_t = 0$ if the price in period t is not an outlier. We then calculate the despiked prices $\{p_t'\}_{t\in\mathcal{T}}$ by subtracting the spikes from the observed prices (i.e., $p_t' = p_t - j_t$). Since the seasonal variation can be identified more accurately after elimination of the spikes, we now fit the above linear regression to the despiked prices and obtain a more refined seasonality model $\{\hat{\psi}_t'\}_{t\in\mathcal{T}}$. We calculate the despiked and deseasonalized prices $\{\rho_t\}_{t\in\mathcal{T}}$ by removing the refined seasonal effect from the despiked prices $\{p_t'\}_{t\in\mathcal{T}}$ (i.e., $\rho_t = p_t' - \hat{\psi}_t'$).

Following Lucia and Schwartz (2002), we model the despiked and deseasonalized price as a stochastic mean-reverting process. We capture

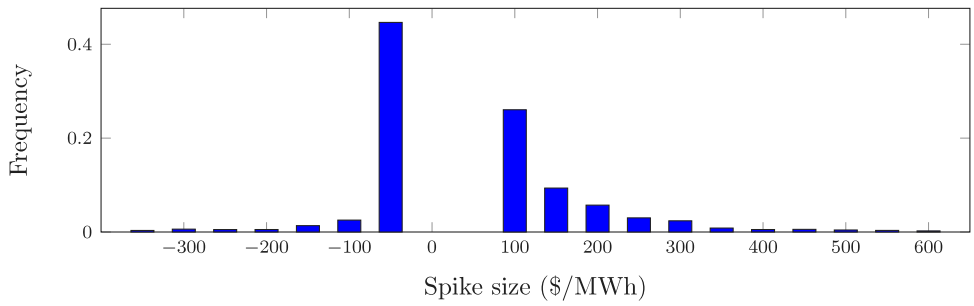

Fig. 3. Empirical distribution of the spikes. The spike range is indeed [−2600, 2500]; the spikes outside the displayed range are omitted due to their low frequencies.

Table 1
Parameter estimates of the despiked price seasonality model.

$\hat{\gamma}_1^{(p)}$	39.7689										
i	1	2	3	4	5	6	7	8	9	10	11
$\hat{\gamma}_{2i}^{(p)}$	19.12	11.37	−2.17	−6.50	−9.76	−10.10	−5.27	−6.00	−8.85	−9.83	−7.11
j	1	2	3	4	5	6					
$\hat{\gamma}_{3j}^{(p)}$	3.74	3.82	4.05	3.87	3.55	1.54					

the mean-reverting behavior via an autoregressive of order one, AR(1), model. Assuming that error terms $\{\epsilon_t\}_{t\in\mathcal{T}}$ are independent standard normal random variables, we formulate the AR(1) process as follows:

$$\rho_t = \left(1-\kappa^{(p)}\right)\rho_{t-1} + \sigma^{(p)}\epsilon_t,\ \forall t,$$

where $\kappa^{(p)}$ is the speed of mean-reversion and $\sigma^{(p)}$ is the volatility of white noise. We have found that the mean absolute error (MAE) of this calibration is $10.02 for the despiked prices. The parameter estimates of the AR(1) process are $\hat{\kappa}^{(p)} = 0.357$ and $\hat{\sigma}^{(p)} = 15.281$. Table 1 exhibits the parameter estimates of the seasonality model. Fig. 3 illustrates the empirical distribution of the spikes. The estimate $\hat{\lambda}$ of the spike occurrence probability is ten percent.

4.2. Time series model for the wind speed

We consider the wind speed data available for Albany, in the State of New York, between the years 2007 and 2012 in which the wind speed is recorded every five minutes. We retrieve this data from NOAA (2019). The average, median, minimum, and maximum values of the wind speed are 8.52, 8.21, 0.05, and 28.67, in m/s, respectively. As we assume hourly periods, we include the wind speed value of every hour of the day in our time series model. Our spectral analysis of the time series indicates the existence of two significant seasonal factors: hourly and daily patterns.

We calibrate our hourly wind speed model via the dynamic harmonic regression with autoregressive integrated moving average (DHR + ARIMA) model (Chen and Rabiti 2017, Zhou et al. 2019): We first fit a linear regression with Fourier terms to our wind speed data to obtain a seasonality model $\{\hat{f}_t\}_{t\in\mathcal{T}}$:

$$f_t = \gamma_0^{(w)} + \gamma_1^{(w)}\cos\left(\frac{2\pi\left(t+\omega_1^{(w)}\right)}{24}\right) + \gamma_2^{(w)}\cos\left(\frac{2\pi\left(\lceil t/24\rceil+\omega_2^{(w)}\right)}{365}\right)$$

where $\lceil . \rceil$ is the ceiling function, $\gamma_0^{(w)}$ is a constant, $\gamma_1^{(w)}$ and $\omega_1^{(w)}$ are the hourly magnitude and phase-shift parameters, and $\gamma_2^{(w)}$ and $\omega_2^{(w)}$ are the daily magnitude and phase-shift parameters, respectively. We calculate the deseasonalized wind speeds $\{\xi_t\}_{t\in\mathcal{T}}$ by removing the seasonal effect from the observed wind speeds $\{w_t\}_{t\in\mathcal{T}}$ (i.e., $\xi_t = w_t - \hat{f}_t$). We then model the deseasonalized wind speed as an AR(1) process as follows:

$$\xi_t = \phi^{(w)}\xi_{t-1} + \sigma^{(w)}\epsilon_t,\ \forall t,$$

where $\phi^{(w)}$ is the autoregressive coefficient and $\sigma^{(w)}$ is the volatility of white noise. We have found that the MAE of our DHR+AR(1) model is only 1.08 m/s. The parameter estimates of the DHR+AR(1) model are $\hat{\gamma}_0^{(w)} = 8.519$, $\hat{\gamma}_1^{(w)} = 1.126$, $\hat{\gamma}_2^{(w)} = 1.74$, $\hat{\omega}_1^{(w)} = 0.002$, $\hat{\omega}_2^{(w)} = -32.431$, $\hat{\phi}^{(w)} = 0.931$, and $\hat{\sigma}^{(w)} = 1.558$.

Finally, we investigate whether there exists any significant correlation between the data sets that we use to model the electricity price and wind speed. We have found that the Pearson correlation coefficient is only 0.031. Hence, constructing independent time series models seems to be benign.

4.3. Discretization for the numerical study

Our time series models in Sections 4.1–4.2 formulate the random component of each exogenous state variable in our MDP as an AR(1) process. This allows us to reduce the computational burden of our MDP: we can redefine the exogenous state tuple in each period t as $I_t = (\xi_t, \rho_t, j_t)$, without requiring the entire historical data in this tuple. We include the spike component of the price in the tuple I_t for calculation of the effective price in period t. For our numerical study, we now provide discrete-state approximations for the continuous-state AR(1) processes embedded in the tuple I_t.

For the electricity price, we characterize the AR(1) process of the random component (i.e., the despiked and deseasonalized price) as a finite-state Markov chain by transforming it into a lattice. A lattice can be defined as a tree with discrete time steps that specifies attainable price levels and their probabilities for each time step. With the estimated parameters $\hat{\kappa}^{(p)}$ and $\hat{\sigma}^{(p)}$, we employ the trinomial lattice method of Hull and White (1994). Specifically, assuming hourly time steps, the price levels can only be multiples of $\sqrt{3}\hat{\sigma}^{(p)}$ and each price level in each period transitions into three possible price levels in the next period. The transition probabilities are chosen to match the first two moments of the continuous distribution of the original AR(1) process (i.e., normal distribution with a mean of zero and a variance of $\hat{\sigma}^{(p)}$). Regarding the number of time steps that should be iterated, we follow the suggestions of Hull and White (1994) and Jaillet et al. (2004), and construct a three-hour trinomial lattice for our AR(1) process. The Markov chain obtained from this lattice has the state space $\mathcal{P} := \{-52.93, -26.47, 0, 26.47, 52.93\}$. The transition matrix of this Markov chain is

$$P^{(p)} = \begin{array}{c} \\ -52.93 \\ -26.47 \\ 0.0 \\ 26.47 \\ 52.93 \end{array} \begin{array}{c} \begin{array}{ccccc} -52.93 & -26.47 & 0.0 & 26.47 & 52.93 \end{array} \\ \begin{pmatrix} .351 & .585 & .065 & 0 & 0 \\ .052 & .539 & .409 & 0 & 0 \\ 0 & .167 & .667 & .167 & 0 \\ 0 & 0 & .409 & .539 & .052 \\ 0 & 0 & .065 & .585 & .351 \end{pmatrix} \end{array}.$$

For the electricity price, we also restrict the spikes to take values from the set $\mathcal{J} := \{-350, -300, \ldots, 550, 600\}$. We compute the probability mass function by approximating the spikes with the closest values in $\mathcal{J}$ and using the empirical distribution of these approximate values. Recall that the spike occurrence probability is ten percent in each period.

$$P^{(w)} = \begin{array}{c} \\ 0 \\ 1 \\ 2 \\ 3 \\ 4 \\ 5 \\ 6 \\ 7 \\ 8 \\ 9 \\ 10 \end{array} \begin{array}{c} \begin{array}{ccccccccccc} 0 & 1 & 2 & 3 & 4 & 5 & 6 & 7 & 8 & 9 & 10 \end{array} \\ \begin{pmatrix} .626 & .206 & .114 & .042 & .010 & .002 & 0 & 0 & 0 & 0 & 0 \\ .391 & .252 & .201 & .107 & .039 & .009 & .002 & 0 & 0 & 0 & 0 \\ .191 & .217 & .251 & .195 & .101 & .035 & .008 & .001 & 0 & 0 & 0 \\ .071 & .133 & .222 & .250 & .188 & .095 & .032 & .007 & .001 & 0 & 0 \\ .019 & .057 & .139 & .227 & .248 & .182 & .090 & .030 & .007 & .001 & 0 \\ .004 & .018 & .062 & .146 & .231 & .246 & .176 & .084 & .027 & .006 & .001 \\ .001 & .004 & .019 & .067 & .153 & .235 & .243 & .169 & .079 & .025 & .006 \\ 0 & .001 & .004 & .021 & .071 & .159 & .239 & .241 & .163 & .075 & .025 \\ 0 & 0 & .001 & .005 & .024 & .076 & .166 & .243 & .241 & .164 & .081 \\ 0 & 0 & 0 & .001 & .006 & .026 & .083 & .177 & .257 & .260 & .191 \\ 0 & 0 & 0 & 0 & .001 & .007 & .031 & .097 & .210 & .317 & .338 \end{pmatrix} \end{array}.$$

Box I.

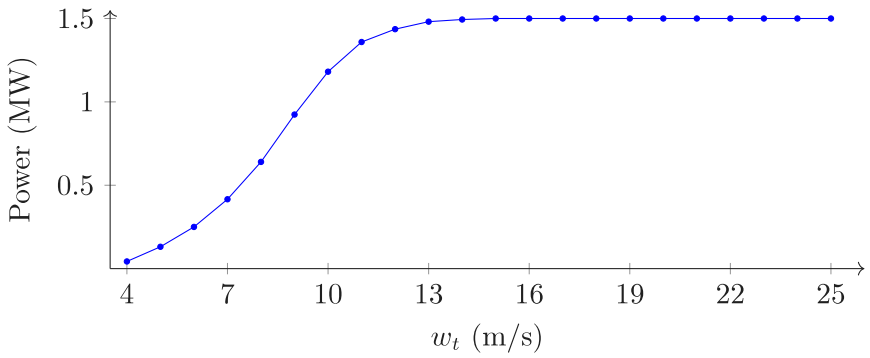

Fig. 4. Power curve of a single GE 1.5-77 turbine (General Electric, 2019).

Since the maximum wind speed observed between 2007 and 2012 is 28.67 m/s, we characterize the AR(1) process of the random component of the wind speed as a Markov chain with the state space $\{0, 1, \ldots, 28\}$. For this state space, we calculate the transition probabilities by following the procedure in Tauchen (1986). In this procedure, we first partition the state space into the evenly spaced intervals $\{(-\infty, 0.5), [0.5, 1.5), \ldots, [26.5, 27.5), (27.5, \infty)\}$ (except the initial and last intervals). We then take the transition probability from one specific state to another state as the probability that the original AR(1) process moves from this specific state to a point in the corresponding next-state interval. In our experiments, we consider a wind power plant with General Electric (GE) 1.5-77 turbines; the power output of each such turbine is determined by the power curve depicted in Fig. 4. The values of the random component greater than nine, combined with the seasonality component that we have found to be always larger than five for our data, yield the same power output. Hence, for computational purposes, we reformulate our Markov chain by reducing its state space to the set $\mathcal{W} := \{0, 1, \ldots, 10\}$ via the state reduction algorithm of Sheskin (1985). The transition matrix of this Markov chain can be seen in Box I.

With the above modifications, we obtain $I_t = (\xi_t, \rho_t, j_t) \in \mathcal{I}_t := \mathcal{W} \times \mathcal{P} \times \mathcal{J}$. In addition, we restrict the amount of energy accumulated in the battery and the amount of energy committed to selling/purchasing to take values from the sets $\mathcal{S} := \{n\zeta_a \in [0, C_S] : n \in \mathbb{Z}\}$ and $\mathcal{Q} := \{k\zeta_a \in [-C_T, \tau C_T] : k \in \mathbb{Z}\}$, respectively, where ζ_a is a prespecified constant. For the discrete-state version of our MDP in Section 3.1, let $\mathbb{U}^D(Q_t, S_t, I_t)$ denote the set of action triplets (q_t, s_t, w_t) that are admissible in state $(Q_t, S_t, I_t) \in \mathcal{Q} \times \mathcal{S} \times \mathcal{I}_t$. The set $\mathbb{U}^D(Q_t, S_t, I_t)$ consists of the set $\{(k\zeta_a, n\zeta_a, m\zeta_a) \in \mathbb{U}(Q_t, S_t, I_t) : k \in \mathbb{Z}, n \in \mathbb{Z}, m \in \mathbb{Z}_+\}$, as well as the extreme points of $\mathbb{U}(Q_t, S_t, I_t)$. Similarly, for our MDP in Section 3.2, let $\hat{\mathbb{U}}^D(Q_t, S_t, I_t)$ denote the set of actions q_t that are admissible in state $(Q_t, S_t, I_t) \in \mathcal{Q} \times \mathcal{S} \times \mathcal{I}_t$. The set $\hat{\mathbb{U}}^D(Q_t, S_t, I_t)$ consists of the set $\{k\zeta_a \in \hat{\mathbb{U}}(Q_t, S_t, I_t) : k \in \mathbb{Z}\}$, as well as the extreme points of $\hat{\mathbb{U}}(Q_t, S_t, I_t)$.

5. Discussion of the numerical results

We consider instances in which the planning horizon spans the first week of August ($T = 168$ hours), the number of GE 1.5-77 turbines is 100, the battery roundtrip efficiency is 0.85, and the transmission line efficiency is 0.97 (Zhou et al., 2019). The negative price occurrence frequency (NPF) takes values from the set $\{0\%, 4.02\%, 7.66\%, 10.96\%, 13.98\%\}$, $C_C = C_D \in \{50, 75, 100\}$ MWh, $C_S \in \{200, 400, 600, 800\}$ MWh, $C_T \in \{100, 200\}$ MWh, $K_p^+ = K_n^- \in \{0.6, 0.7, 0.8, 0.9\}$, and $K_n^+ = K_p^- \in \{1.1, 1.2, 1.3, 1.4\}$. The observed NPF is 4.02% in our time series model for the price. We obtain the other four values of NPF by multiplying the numbers of negative spike occurrences with certain constants. In all instances, the discretization parameter ζ_a is 25 MWh, the initial storage level S_1 is the closest state to $C_S/2$, the initial commitment level Q_1 is zero, and the initial exogenous state $I_1 = (\xi_1, \rho_1, j_1)$ is (5,0,0). We solved the recursion of our MDP to optimality in each instance, calculating the following metrics:

- The expected total cash flow in million dollars (TCF),
- The expected total amount of wind energy curtailed in MWh (WEC),
- The expected total negative imbalance in MWh (NI),
- The expected total positive imbalance in MWh (PI), and
- The expected total imbalance (deviation) in MWh (ED).

We label the problem setting in Section 3.1 as 'ID' (the initials of 'intentional deviation') and the problem setting in Section 3.2 as 'UD' (the initials of 'unintentional deviation'). We also consider two other settings that are the special cases of ID and UD with no battery. We label the problem setting in Section 3.1 with $C_S = 0$ as 'ID-NB' (ID

Table 2
Numerical results when $K_p^+ = K_n^- = 0.9$, $K_n^+ = K_p^- = 1.1$, and NPF = 4.02%.

Setting	C_T	$C_C = C_D$	C_S	TCF	WEC	NI	PI	ED
ID	100	50	200	0.605	2460	2643	395	3038
			400	0.631	2077	2797	313	3109
			600	0.643	1847	2784	279	3062
			800	0.651	1670	2709	261	2970
		75	200	0.616	2520	2931	359	3290
			400	0.648	2162	3220	242	3462
			600	0.665	1949	3304	189	3493
			800	0.676	1777	3283	160	3443
		100	200	0.619	2495	2995	350	3345
			400	0.653	2134	3303	232	3535
			600	0.671	1937	3388	179	3567
			800	0.682	1786	3363	150	3514
	200	50	200	0.746	613	4365	1201	5566
			400	0.774	614	4585	1183	5768
			600	0.788	614	4742	1244	5986
			800	0.797	614	4743	1252	5995
		75	200	0.775	614	5263	951	6214
			400	0.817	616	5906	1234	7140
			600	0.840	619	6113	1304	7418
			800	0.855	618	6290	1339	7628
		100	200	0.795	615	6231	1070	7301
			400	0.848	616	7204	1235	8439
			600	0.879	619	7469	1327	8796
			800	0.899	620	7653	1380	9033
UD	100	50	200	0.540	1769	844	0	844
			400	0.562	1318	611	0	611
			600	0.575	1034	535	0	535
			800	0.584	836	512	0	512
		75	200	0.542	1777	660	0	660
			400	0.567	1313	386	0	386
			600	0.582	1017	275	0	275
			800	0.592	811	224	0	224
		100	200	0.543	1779	646	0	646
			400	0.569	1312	357	0	357
			600	0.584	1011	237	0	237
			800	0.595	799	175	0	175
	200	50	200	0.623	258	683	0	683
			400	0.637	300	611	0	611
			600	0.646	320	634	0	634
			800	0.653	328	665	0	665
		75	200	0.630	156	502	0	502
			400	0.651	181	446	0	446
			600	0.664	204	465	0	465
			800	0.673	220	493	0	493
		100	200	0.633	113	496	0	496
			400	0.658	120	374	0	374
			600	0.675	135	366	0	366
			800	0.687	150	378	0	378

and the initials of 'no battery') and the problem setting in Section 3.2 with $C_S = 0$ as 'UD-NB' (UD and the initials of 'no battery'). In this section, we examine the effects of system components and market characteristics on TCF, WEC, NI, PI, and ED. In Section 5.1, we vary only the values of $C_C = C_D$, C_S, and C_T. In Section 5.2, we vary only the values of $K_p^+ = K_n^-$ and $K_n^+ = K_p^-$. In Section 5.3, we vary only the value of NPF.

5.1. The impact of the size of system components

In this section, we examine the effects of the battery's energy capacity (C_S) and charging/discharging capacity ($C_C = C_D$), and the transmission line capacity (C_T) on the values of TCF, WEC, NI, PI, and ED when $K_p^+ = K_n^- = 0.9$, $K_n^+ = K_p^- = 1.1$, and NPF= 4.02%. See Table 2 and Fig. 5.

We observe from Table 2 that TCF increases with C_S, $C_C = C_D$, and C_T for both ID and UD. The benefit of an additional battery capacity diminishes as the battery becomes larger in capacity and thus the transmission line capacity becomes more binding. We also observe that TCFs are higher in ID than in UD, as expected from Proposition 1. The capacity levels have a greater impact on TCF in ID than in UD because the battery in ID can be used strategically to make more profit. In addition, we note from Table 2 that NIs are higher than PIs for ID. When the producer committed to selling energy to the market, selling less than her commitment in real-time may provide a greater return than selling more than her commitment, since selling more is likely to reduce the battery level more. When the producer committed to purchasing energy from the market to benefit from the negative/low prices, purchasing more than her commitment in real-time provides a greater return than purchasing less than her commitment. Therefore, the producer tends to experience negative imbalances more than positive imbalances. Finally, both NIs and PIs increase with the transmission line capacity.

Table 2 also shows for ID that an increase in C_S may lead to a slight decrease in ED when C_T and $C_C = C_D$ are low, whereas it leads to an increase in ED when C_T or $C_C = C_D$ is high. The maximum amount of energy committed to selling or purchasing is constrained by the transmission line and battery charging/discharging capacities. Having a large storage capacity gives the flexibility to better meet commitments and also deviate from commitments more substantially. When C_T and $C_C = C_D$ are low, the producer better meets her commitments with an increase in C_S, thanks to the constrained commitment levels. On the other hand, when C_T or $C_C = C_D$ is high, the producer can deviate from her commitments more substantially with an increase in C_S, due to the unconstrained commitment levels. For UD, however, increasing C_S reduces ED in many cases and only slightly raises ED in the other cases. This is because the producer in UD should meet her commitments as much as possible; she may only experience negative imbalances, possibly due to the battery's capacity constraints. The decrease in ED is more significant when the transmission line capacity is low, that is, when the commitment decisions are more restricted.

We observe from Fig. 5 that when the transmission line capacity is low (the left plots in Fig. 5), an increase in C_S leads to a decrease in WEC in both ID and UD. Since the low transmission line capacity limits the amount of energy that can be sold in real-time, a battery with larger energy capacity helps the producer store more of the excess wind energy, reducing the curtailment amount. When the transmission line capacity is high (the right plots in Fig. 5), on the other hand, WECs in ID and UD are not affected much by an increase in C_S. Since the high transmission line capacity allows the producer to sell a large amount of the available wind energy, increasing the battery's energy capacity has no significant impact on the curtailment amounts.

5.2. The impact of imbalance pricing parameters

In this section, we examine the effects of the imbalance pricing parameters on the values of TCF, WEC, NI, PI, and ED when $C_S = 400$ MWh (for ID and UD), $C_C = C_D = 50$ MWh (for ID and UD), $C_T = 200$ MWh, and NPF = 4.02%. See Tables 3–4 and Figs. 6–7.

We first note that a decrease in $K_p^+(K_n^-)$ and an increase in $K_n^+(K_p^-)$ improve the effectiveness of the imbalance pricing mechanism, while draining the producer's profit. We observe from Tables 3 and 4 that having a battery brings a financial benefit to the producer and this benefit is lower under smaller penalties (e.g., $K_p^+ = 0.9$ and $K_n^+ = 1.1$). We also observe that TCF decreases in ID and ID-NB, but only slightly in UD and UD-NB, as $K_p^+(K_n^-)$ decreases. The impact of K_p^+ in UD and UD-NB is not significant since the positive imbalance is not observed in UD and UD-NB. Another observation is that TCF decreases in ID, ID-NB, and UD-NB, yet only slightly in UD, as $K_n^+(K_p^-)$ increases. Since the producers in ID and ID-NB intentionally cause an energy imbalance, their profits are affected by the changes in the imbalance pricing parameters. The producers in UD and UD-NB are vulnerable to negative imbalances, but the profit of the producer in UD is quite

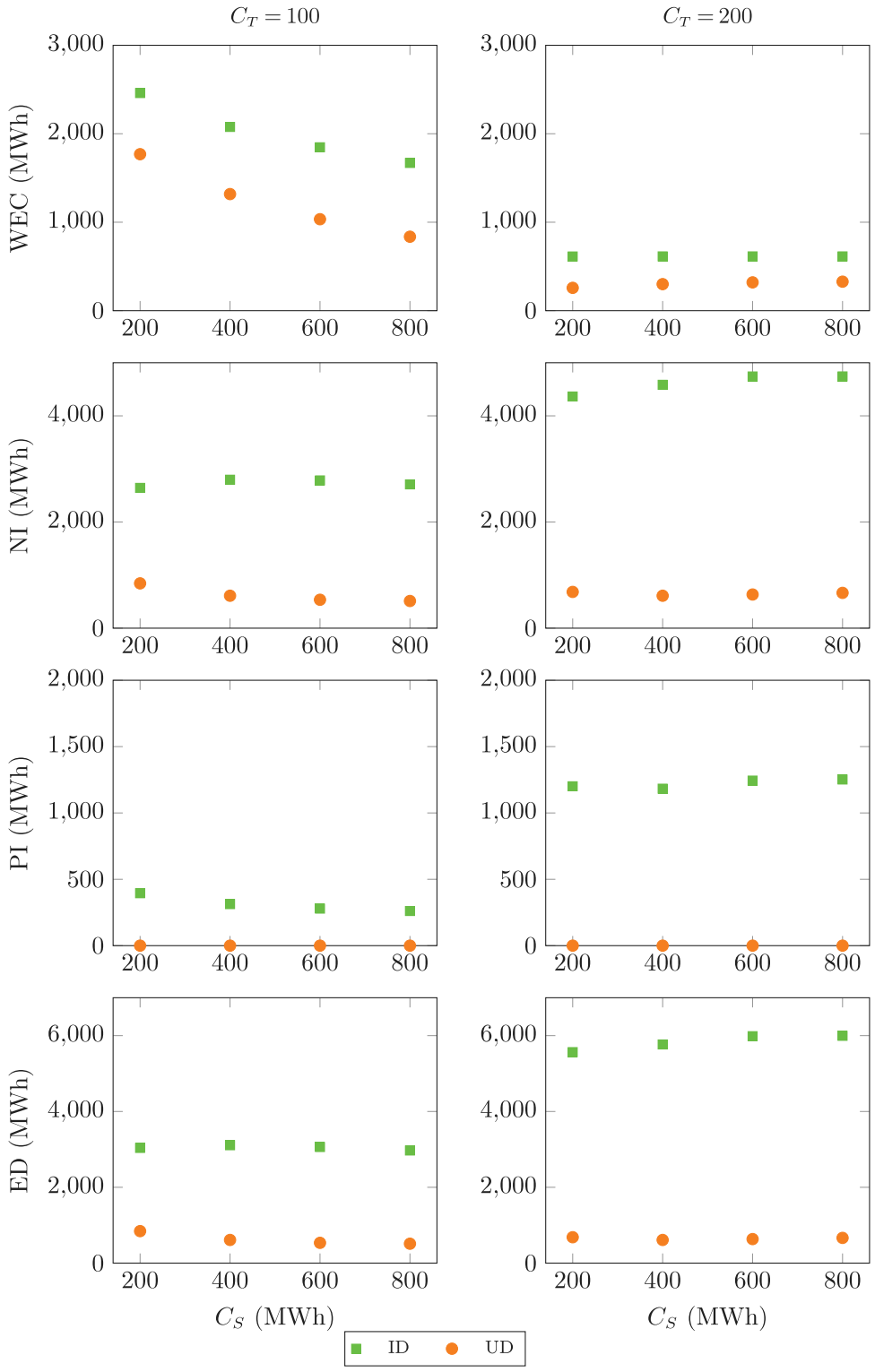

Fig. 5. WEC, NI, PI, and ED vs. C_S when $K_p^+ = K_n^- = 0.9$, $K_n^+ = K_p^- = 1.1$, $C_C = C_D = 50$ MWh, and NPF = 4.02%.

robust to the changes in $K_n^+(K_p^-)$ as she uses the battery to minimize deviations from her commitments.

We observe from Fig. 6 that WEC remains similar in UD, but increases in UD-NB, as $K_n^+(K_p^-)$ increases. When $K_n^+(K_p^-)$ is large, the producer in UD-NB prefers to commit to selling small amounts of energy to avoid any negative imbalance, leading to large curtailment amounts. However, the producer in UD can still commit to selling significant amounts of energy as she uses the battery as a back-up source. We also observe that WECs in ID and ID-NB are not affected by the change in the imbalance pricing parameters. This is because the producers in ID and ID-NB can always sell the excess wind energy as long as the transmission line capacity allows.

The effect of imbalance pricing parameters on ED in ID and ID-NB changes according to the producer's imbalance tendency. First, we note from Table 3 that ED in ID decreases as K_n^+ increases, while it may increase for small values of K_n^+ as K_p^+ decreases. A higher penalty

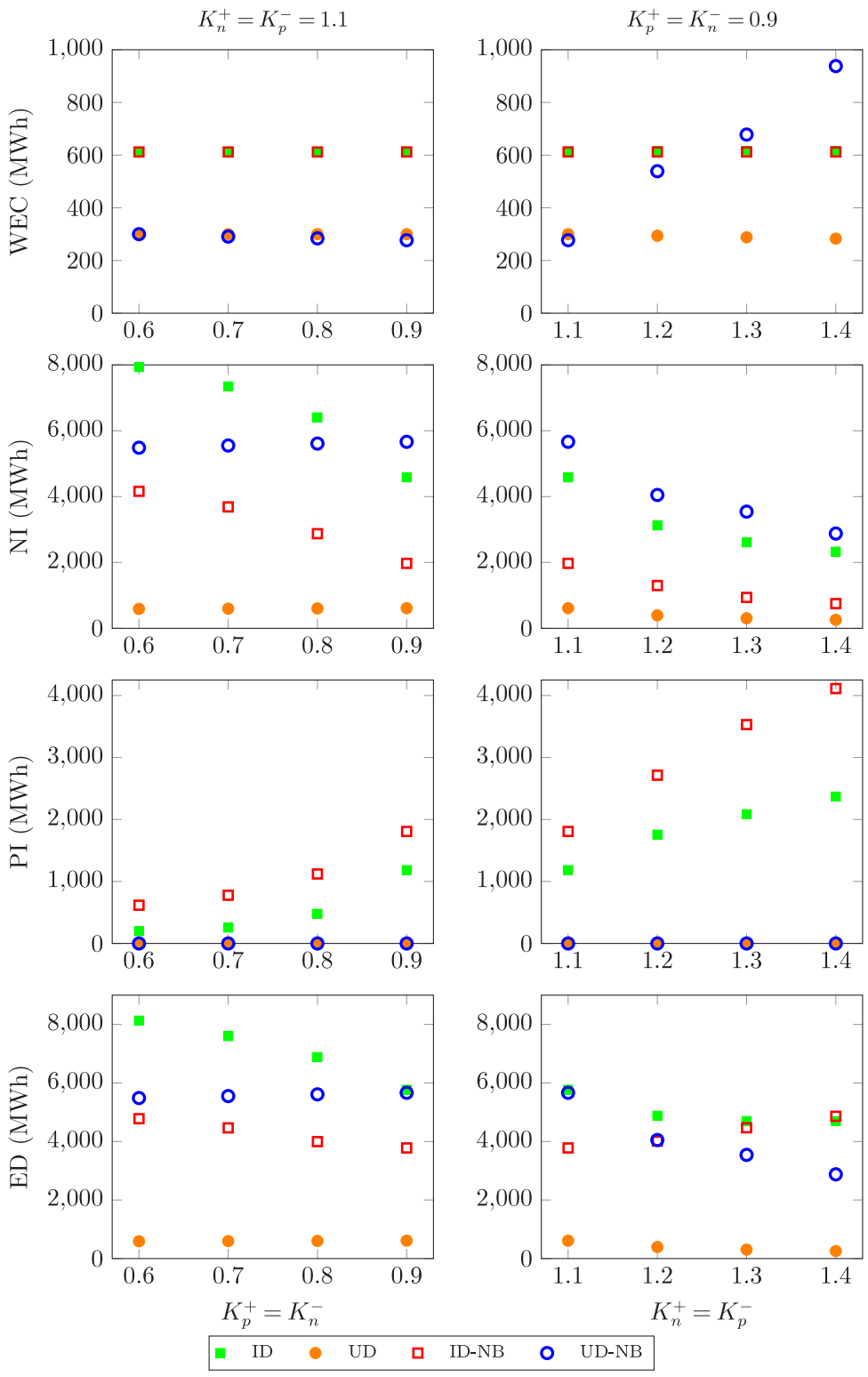

Fig. 6. WEC, NI, PI, and ED vs. $K_p^+ = K_n^-$ and $K_p^+ = K_n^-$ when $C_S = 400$ MWh, $C_C = C_D = 50$ MWh, $C_T = 200$ MWh, and NPF = 4.02%.

for negative (positive) imbalance encourages the producer in ID to stay in positive (negative) imbalance more than in negative (positive) imbalance. Since the producer in ID is more inclined to cause negative imbalances, an increase in K_n^+ leads to a more significant drop in NI (compared to the increase in PI), and thus her total deviation decreases. However, for small values of K_n^+, she experiences a greater increase in NI than a decrease in PI as K_p^+ decreases, leading to an increase in ED. Second, we note from Table 3 that ED in ID-NB tends to decrease for small values of K_p^+, while it tends to increase for large values of K_p^+, as K_n^+ increases. The producer in ID-NB is more conservative in her commitment decisions, causing positive imbalances more as she can still make a profit if the available wind energy is large enough. A higher penalty for negative imbalance makes the producer much more conservative in her commitment decisions. The decrease in NI

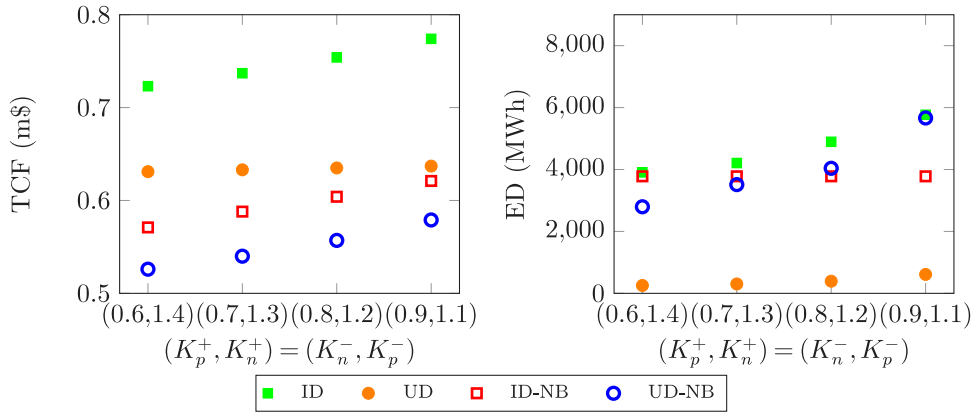

Fig. 7. TCF and ED vs. $K_p^+ = K_n^-$ and $K_n^+ = K_p^-$ when $C_S = 400$ MWh, $C_C = C_D = 50$ MWh, $C_T = 200$ MWh, and NPF = 4.02%.

Table 3
Numerical results for ID and ID-NB when $C_S = 400$ MWh, $C_C = C_D = 50$ MWh, $C_T = 200$ MWh, and NPF = 4.02%.

Setting	$K_p^+ = K_n^-$	$K_n^+ = K_p^-$	TCF	WEC	NI	PI	ED
ID	0.6	1.1	0.747	612	7934	199	8133
		1.2	0.734	612	5202	328	5529
		1.3	0.727	612	3966	414	4380
		1.4	0.723	613	3436	472	3908
	0.7	1.1	0.754	612	7345	256	7601
		1.2	0.743	612	4718	434	5152
		1.3	0.737	613	3647	562	4209
		1.4	0.734	613	3239	647	3886
	0.8	1.1	0.763	612	6407	479	6886
		1.2	0.754	613	4051	843	4895
		1.3	0.750	613	3221	1044	4265
		1.4	0.747	614	2926	1196	4121
	0.9	1.1	0.774	614	4585	1183	5768
		1.2	0.769	615	3126	1755	4881
		1.3	0.766	616	2612	2085	4697
		1.4	0.764	616	2327	2370	4697
ID-NB	0.6	1.1	0.600	612	4161	617	4779
		1.2	0.588	612	2874	1121	3996
		1.3	0.578	612	2399	1428	3827
		1.4	0.571	612	1973	1807	3780
	0.7	1.1	0.606	612	3687	778	4465
		1.2	0.595	612	2551	1317	3869
		1.3	0.588	612	1973	1807	3780
		1.4	0.582	612	1644	2177	3821
	0.8	1.1	0.612	612	2874	1121	3996
		1.2	0.604	612	1973	1807	3780
		1.3	0.599	612	1511	2359	3870
		1.4	0.595	612	1299	2715	4013
	0.9	1.1	0.621	612	1973	1807	3780
		1.2	0.616	612	1299	2715	4013
		1.3	0.613	612	938	3531	4469
		1.4	0.612	612	750	4113	4862

Table 4
Numerical results for UD and UD-NB when $C_S = 400$ MWh, $C_C = C_D = 50$ MWh, $C_T = 200$ MWh, and NPF = 4.02%.

Setting	$K_p^+ = K_n^-$	$K_n^+ = K_p^-$	TCF	WEC	NI	PI	ED
UD	0.6	1.1	0.637	300	590	0	590
		1.2	0.635	294	387	0	387
		1.3	0.633	288	302	0	302
		1.4	0.631	283	254	0	254
	0.7	1.1	0.637	300	596	0	596
		1.2	0.635	294	389	0	389
		1.3	0.633	288	303	0	303
		1.4	0.631	283	255	0	255
	0.8	1.1	0.637	300	604	0	604
		1.2	0.635	294	392	0	392
		1.3	0.633	288	305	0	305
		1.4	0.631	283	257	0	257
	0.9	1.1	0.637	300	611	0	611
		1.2	0.635	294	394	0	394
		1.3	0.633	288	306	0	306
		1.4	0.631	283	258	0	258
UD-NB	0.6	1.1	0.576	300	5485	0	5485
		1.2	0.556	557	3976	0	3976
		1.3	0.540	698	3486	0	3486
		1.4	0.526	975	2796	0	2796
	0.7	1.1	0.577	291	5552	0	5552
		1.2	0.557	546	4022	0	4022
		1.3	0.540	689	3512	0	3512
		1.4	0.526	962	2825	0	2825
	0.8	1.1	0.578	284	5611	0	5611
		1.2	0.557	542	4039	0	4039
		1.3	0.541	682	3531	0	3531
		1.4	0.527	948	2857	0	2857
	0.9	1.1	0.579	277	5664	0	5664
		1.2	0.558	539	4050	0	4050
		1.3	0.541	678	3543	0	3543
		1.4	0.527	938	2878	0	2878

dominates the increase in PI for small values of K_p^+, while the reverse is true for large values of K_p^+.

We observe from Tables 3 and 4 that ED in ID is greater than in UD, UD-NB, and ID-NB. Having a battery reduces the energy imbalance in the market if the producer uses it to better fulfill her commitments (from UD-NB to UD). Having a battery increases the energy imbalance if the producer uses it to support her intentional deviations (from UD to ID or from ID-NB to ID). Since the producer in UD aims to fulfill her commitments, ED in UD is not affected much by the changes in the imbalance pricing parameters, compared to ID and UD-NB. Finally, we observe from Fig. 7 that ED in ID-NB is not affected by the changes in the imbalance pricing parameters as long as they are symmetric, while TCF in ID-NB is affected significantly by these changes. The setting in ID-NB under symmetric imbalance pricing parameters can be viewed as a newsvendor-type inventory problem where the unit costs of overstocking and understocking are equal to each other so that the critical fractile is always 0.5.

5.3. The impact of negative electricity prices

In this section, we examine the effects of the negative price occurrence frequency on the values of TCF, WEC, NI, PI, and ED when $C_S = 400$ MWh (for ID and UD), $C_C = C_D = 50$ MWh (for ID and UD), $C_T = 200$ MWh, $K_p^+ = K_n^- = 0.9$, and $K_n^+ = K_p^- = 1.1$. See Fig. 8.

We observe that TCF decreases as NPF grows. This is because the average electricity price is lower when NPF is larger. An important

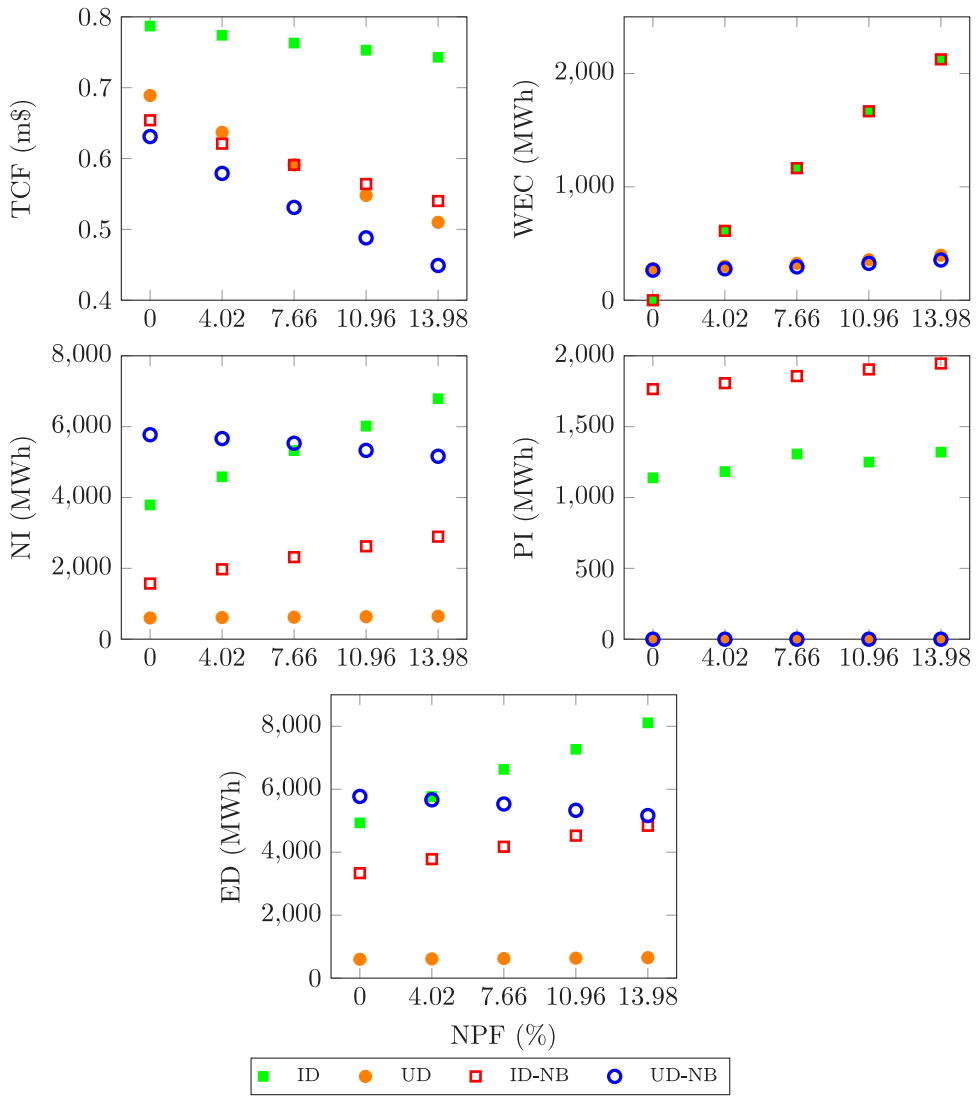

Fig. 8. TCF, WEC, NI, PI, and ED vs. NPF when $K_p^+ = K_n^- = 0.9$, $K_n^+ = K_p^- = 1.1$, $C_S = 400$ MWh (for ID and UD), $C_C = C_D = 50$ MWh (for ID and UD), and $C_T = 200$ MWh.

observation is that having a battery for intentional deviations becomes much more valuable as NPF grows. We also note that for small NPF values, TCF in UD is larger than TCF in ID-NB. For large NPF values, however, TCF in UD is smaller than TCF in ID-NB. Under nonnegative electricity prices, the producers in ID and ID-NB do not curtail the excess wind energy (as long as the transmission line capacity allows) since there is still a positive economic return when they sell the excess energy to the market at a lower price than the market price. Although the producers in UD and UD-NB could be better off by selling the excess energy under nonnegative prices, they curtail the excess wind energy to reduce deviations from their commitments, as imposed by the problem setting in Section 3.2. As NPF grows, WEC increases in ID and ID-NB more significantly than in UD and UD-NB. For the producer in ID, the incentive to keep the battery level low to benefit from the negative prices dominates the incentive to store the excess wind energy in the battery. The producer in ID-NB can benefit from the negative prices by selling energy less than her commitment, leading to large curtailment amounts. This also explains why ID-NB can be more profitable than UD when NPF is large.

We observe that ED increases in ID and ID-NB, decreases in UD-NB, and remains similar in UD, as NPF grows. The producer in ID has an incentive to purchase energy at negative prices to sell it in future periods with high prices by deviating from her commitments (leading to greater NIs). She also has an incentive to discharge the battery by selling energy more than her commitment at nonnegative prices to purchase energy in future periods with negative prices (leading to greater PIs). The producer in ID-NB has an incentive to sell energy less than her commitment at negative prices (leading to greater NIs). She also has an incentive to commit to selling less energy when NPF is larger so that the positive imbalances are larger in periods with positive prices (leading to greater PIs). The producer in UD-NB becomes more conservative in her commitment decisions to suffer less from a large NPF, thereby meeting her commitments better. Finally, although the producer in UD wants to take advantage of the negative prices by committing to purchasing more energy, the increase in NPF does not have a significant effect on her deviations since her primary goal is to fulfill her commitments as much as possible with the help of the battery.

5.4. The impact of wind availability

Finally, we examine the effects of season and location on our key observations in Sections 5.1–5.3, by extending all of our experiments in Sections 5.1–5.3 to the month of January in the city of Albany and

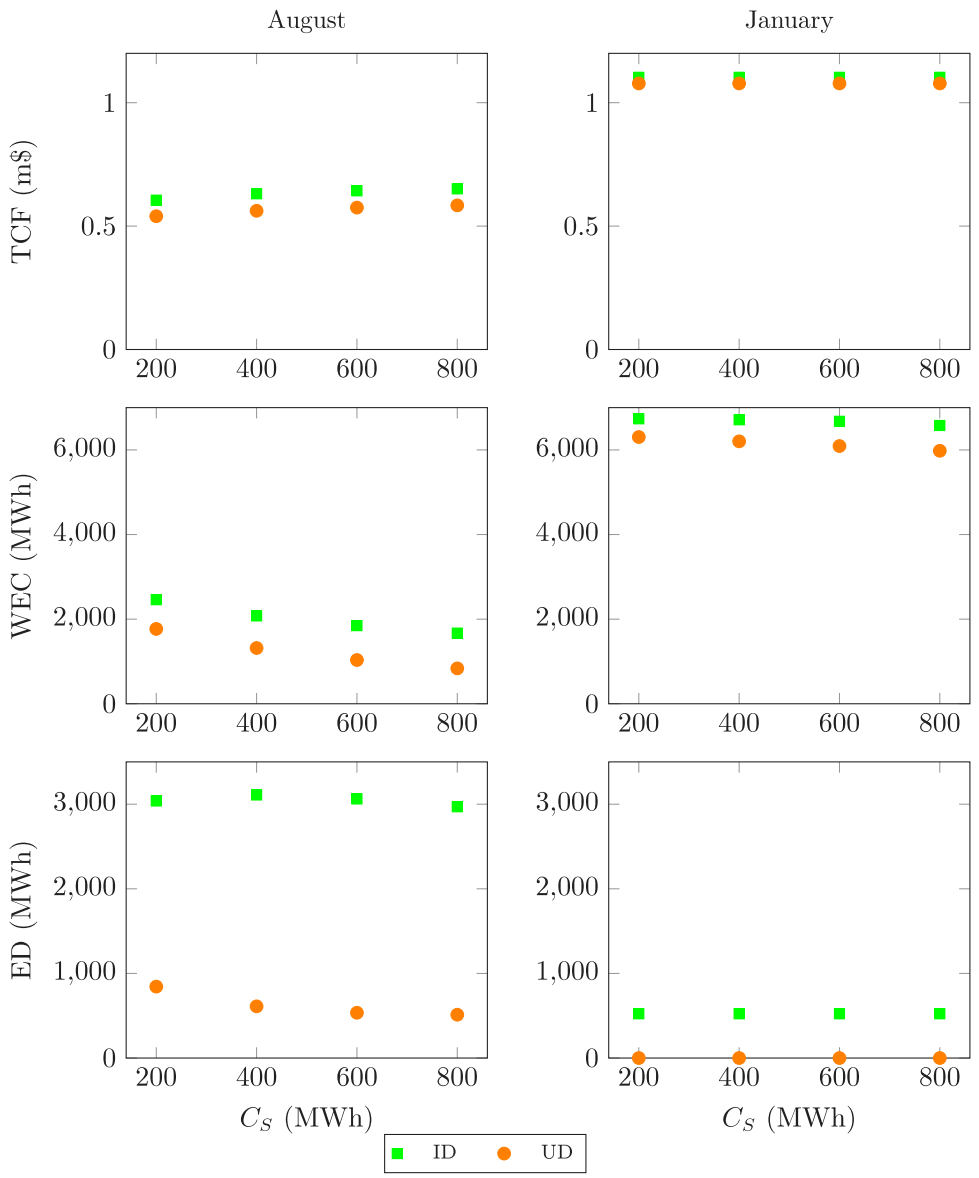

Fig. 9. TCF, WEC, and ED vs. C_S when $K_p^+ = K_n^- = 0.9$, $K_n^+ = K_p^- = 1.1$, $C_C = C_D = 50$ MWh, $C_T = 100$ MWh, NPF = 4.02% in August, and NPF = 1.61% in January.

to the city of Buffalo in the month of August. Recall that we performed our earlier experiments for the month of August in the city of Albany.

Our time series model for the city of Albany implies that the months of August and January exhibit distinct features in terms of wind speed. The average, median, minimum, and maximum values of the wind speed in August are 6.76, 6.54, 0.06, and 27.97, in m/s, respectively. The average, median, minimum, and maximum values of the wind speed in January are 9.98, 9.94, 0.05, and 27.01, in m/s, respectively. We have found that our key insights related to the impacts of imbalance pricing parameters and negative electricity prices remain valid in January. While our key insights related to the impact of the size of system components remain valid when transmission line capacity is high ($C_T = 200$), we observe a few notable differences when transmission line capacity is low ($C_T = 100$), as can be seen from Fig. 9. Since there is a better wind availability in January than in August, the transmission line capacity becomes even more binding in January when $C_T = 100$ so that TCF and ED are unaffected by changes in the storage capacity for ID and UD. For the same reason, WEC declines more slowly in January than in August as C_S grows. We also note that the producer in UD can always fulfill her commitments. This is because the producer always commits to selling the maximum amount of energy that the transmission line capacity allows and is able to supply this amount of energy in real-time thanks to high wind availability.

We next consider the wind speed data available for Buffalo, in the State of New York, between the years 2007 and 2012 in which the wind speed is recorded every five minutes. We retrieve this data from NOAA (2019). The average, median, minimum, and maximum values of the wind speed in August are 6.01, 5.65, 0.08, and 20.10, in m/s, respectively. We have found that the MAE of our DHR+AR(1) model is only 0.86 m/s. The parameter estimates of the DHR+AR(1) model are $\hat{\gamma}_0^{(w)} = 7.587$, $\hat{\gamma}_1^{(w)} = 0.917$, $\hat{\gamma}_2^{(w)} = 1.485$, $\hat{\omega}_1^{(w)} = -0.832$, $\hat{\omega}_2^{(w)} = -20.627$, $\hat{\phi}^{(w)} = 0.938$, and $\hat{\sigma}^{(w)} = 1.200$. Our key insights related to the impacts of imbalance pricing parameters and negative electricity prices continue to hold in Buffalo. Since there is a lower wind availability in Buffalo than in Albany, the transmission line capacity becomes less binding in Buffalo when $C_T = 100$ so that our key observations for Buffalo when $C_T = 100$ are similar to those for Albany when $C_T = 200$.

6. Concluding remarks

We have studied the energy commitment, generation, and storage problem for an energy system that consists of a wind power plant and a

battery. We consider the following two possible settings: (i) The battery can be used to support intentional deviations from commitments or (ii) it should be used to minimize such deviations. We model these problems as an MDP by taking into account the electricity price and wind uncertainties. We construct data-calibrated time series models for the electricity price and wind speed, which we incorporate into our MDP formulations. We numerically examine the effects of system components, imbalance pricing parameters, and negative prices on the producer's profits, curtailment decisions, and imbalance tendencies for each problem setting.

Our numerical results for Albany in August show that behaving strategically in commitment fulfillment decisions improves the wind power producer's profit by 9.5%, while increasing the imbalance amount by 7.3%, on average, in the absence of a battery (UD-NB vs. ID-NB). Using the battery as a strategic tool to intentionally deviate from commitments rather than restricting its use to fulfillment of commitments improves the producer's profit by 20.1%, while increasing the imbalance amount by ten times (UD vs. ID). The existence of a battery increases the profit and imbalance amount of the producer making intentional deviations by 26.1% and 24.3%, respectively (ID vs. ID-NB). Although the existence of a battery increases the profit of the producer aiming to fulfill her commitments by 14.4%, it reduces her imbalance amount by 90.0% (UD vs. UD-NB). Our results may guide the wind power producers in their assessment of the battery adoption decisions as well as the system operators in their understanding of the producers' behavior in different environments.

Future research may characterize the optimal policy structure for the energy commitment, generation, and storage problem of the producer. Future work may also consider alternative renewable energy sources (e.g., wind speed, solar irradiation, and streamflow) to study their joint operations with a storage unit. Another direction for future research is to extend our MDP formulations and their analysis to sequential markets such as day-ahead, intraday, and balancing markets. Lastly, it might be interesting to examine the roles of different balancing rules such as dual-pricing and imbalance subsidies in the producer's profits and operations.

Data availability

We have used publicly available data sets.

Acknowledgments

The authors thank the editor and two anonymous referees for their constructive comments and suggestions. Dr. Kocaman was supported by the BAGEP Award of the Science Academy, Turkey.

Appendix. Proof of Proposition 1

Note that $v_T^*(Q_T, S_T, I_T) = \hat{v}_T^*(Q_T, S_T, I_T) = 0$. Assuming $v_{t+1}^*(Q_{t+1}, S_{t+1}, I_{t+1}) \geq \hat{v}_{t+1}^*(Q_{t+1}, S_{t+1}, I_{t+1})$, we show $v_t^*(Q_t, S_t, I_t) \geq \hat{v}_t^*(Q_t, S_t, I_t)$. Let $\hat{\mathbb{U}}^F(Q_t, S_t, I_t) = \{(q_t, s_t, w_t) \in \mathbb{U}(Q_t, S_t, I_t) : s_t = \hat{s}_t, w_t = \hat{w}_t, \text{ and } q_t \in \hat{\mathbb{U}}(Q_t, S_t, I_t)\}$. Since $v_{t+1}^*(Q_{t+1}, S_{t+1}, I_{t+1}) \geq \hat{v}_{t+1}^*(Q_{t+1}, S_{t+1}, I_{t+1})$ and $\hat{\mathbb{U}}^F(Q_t, S_t, I_t) \subseteq \mathbb{U}(Q_t, S_t, I_t)$,

$$
\begin{aligned}
& v_t^*(Q_t, S_t, I_t) \\
&= \max_{(q_t, s_t, w_t) \in \mathbb{U}(Q_t, S_t, I_t)} \left\{ R(Q_t, I_t, E(s_t, w_t)) + \mathbb{E}_{I_{t+1}|I_t} \left[v_{t+1}^*(q_t, S_{t+1}, I_{t+1}) \right] \right\} \\
&\geq \max_{(q_t, s_t, w_t) \in \mathbb{U}(Q_t, S_t, I_t)} \left\{ R(Q_t, I_t, E(s_t, w_t)) + \mathbb{E}_{I_{t+1}|I_t} \left[\hat{v}_{t+1}^*(q_t, S_{t+1}, I_{t+1}) \right] \right\} \\
&\geq \max_{(q_t, s_t, w_t) \in \hat{\mathbb{U}}^F(Q_t, S_t, I_t)} \left\{ R(Q_t, I_t, E(s_t, w_t)) + \mathbb{E}_{I_{t+1}|I_t} \left[\hat{v}_{t+1}^*(q_t, S_{t+1}, I_{t+1}) \right] \right\} \\
&= \max_{q_t \in \hat{\mathbb{U}}(Q_t, S_t, I_t)} \left\{ R(Q_t, I_t, E(Q_t, S_t, I_t)) + \mathbb{E}_{I_{t+1}|I_t} \left[\hat{v}_{t+1}^*(q_t, S_{t+1}, I_{t+1}) \right] \right\} \\
&= \hat{v}_t^*(Q_t, S_t, I_t).
\end{aligned}
$$

Hence $v_t^*(Q_t, S_t, I_t) \geq \hat{v}_t^*(Q_t, S_t, I_t)$, $\forall t$, implying that $v_1^*(Q_1, S_1, I_1) \geq \hat{v}_1^*(Q_1, S_1, I_1)$.

References

Al-Swaiti, M.S., Al-Awami, A.T., Khalid, M.W., 2017. Co-optimized trading of wind-thermal-pumped storage system in energy and regulation markets. Energy 138, 991–1005.

Bajwa, M., Cavicchi, J., 2017. Growing evidence of increased frequency of negative electricity prices in US wholesale electricity markets. In: IAEE Energy Forum, vol. 37.

Bird, L., Lew, D., Milligan, M., Carlini, E.M., Estanqueiro, A., Flynn, D., Gomez-Lazaro, E., Holttinen, H., Menemenlis, N., Orths, A., et al., 2016. Wind and solar energy curtailment: A review of international experience. Renew. Sustain. Energy Rev. 65, 577–586.

Boomsma, T.K., Juul, N., Fleten, S.-E., 2014. Bidding in sequential electricity markets: The Nordic case. European J. Oper. Res. 238 (3), 797–809.

Brijs, T., Geth, F., De Jonghe, C., Belmans, R., 2019. Quantifying electricity storage arbitrage opportunities in short-term electricity markets in the CWE region. J. Energy Storage 25, 100899.

CAISO, 1998. Chapter 4. Real-time energy market. https://www.caiso.com/Documents/Chapter4_1998AnnualReport_MarketIssuesandPerformance.pdf (Accessed 8 June 2022).

CAISO, 2007. Attachment D – Benchmarking against NYISO, PJM, and ISO-NE. https://www.caiso.com/Documents/AttachmentD-BenchmarkingAgainstNYISO_PJMandISO-NE.pdf (Accessed 8 June 2022).

CAISO, 2013. CAISO annual market report on market issues and performance. https://www.transmissionhub.com/wp-content/uploads/2018/12/California-ISO-APR-28-2014.pdf (Accessed June 8, 2022).

Castronuovo, E.D., Usaola, J., Bessa, R., Matos, M., Costa, I., Bremermann, L., Lugaro, J., Kariniotakis, G., 2014. An integrated approach for optimal coordination of wind power and hydro pumping storage. Wind Energy 17 (6), 829–852.

Chaves-Ávila, J.P., Hakvoort, R.A., Ramos, A., 2014. The impact of European balancing rules on wind power economics and on short-term bidding strategies. Energy Policy 68, 383–393.

Chen, J., Rabiti, C., 2017. Synthetic wind speed scenarios generation for probabilistic analysis of hybrid energy systems. Energy 120, 507–517.

Dadashi, M., Zare, K., Seyedi, H., Shafie-khah, M., 2022. Coordination of wind power producers with an energy storage system for the optimal participation in wholesale electricity markets. Int. J. Electr. Power Energy Syst. 136, 107672.

De Jonghe, C., Delarue, E., Belmans, R., D'haeseleer, W., 2011. Determining optimal electricity technology mix with high level of wind power penetration. Appl. Energy 88 (6), 2231–2238.

Díaz, G., Coto, J., Gómez-Aleixandre, J., 2019. Optimal operation value of combined wind power and energy storage in multi-stage electricity markets. Appl. Energy 235, 1153–1168.

Ding, H., Hu, Z., Song, Y., 2014. Rolling optimization of wind farm and energy storage system in electricity markets. IEEE Trans. Power Syst. 30 (5), 2676–2684.

Ding, H., Pinson, P., Hu, Z., Song, Y., 2015. Integrated bidding and operating strategies for wind-storage systems. IEEE Trans. Sustain. Energy 7 (1), 163–172.

Ederer, N., 2015. The market value and impact of offshore wind on the electricity spot market: Evidence from Germany. Appl. Energy 154, 805–814.

EIA, 2020. Large battery systems are often paired with renewable energy power plants. https://www.eia.gov/todayinenergy/detail.php?id=43775 (Accessed 3 May 2022).

Eicke, A., Ruhnau, O., Hirth, L., 2021. Electricity balancing as a market equilibrium: An instrument-based estimation of supply and demand for imbalance energy. Energy Econ. 102, 105455.

Elshurafa, A.M., 2020. The value of storage in electricity generation: A qualitative and quantitative review. J. Energy Storage 32, 101872.

Finnah, B., Gönsch, J., 2021. Optimizing trading decisions of wind power plants with hybrid energy storage systems using backwards approximate dynamic programming. Int. J. Prod. Econ. 238, 108155.

Finnah, B., Gönsch, J., Ziel, F., 2022. Integrated day-ahead and intraday self-schedule bidding for energy storage systems using approximate dynamic programming. European J. Oper. Res. 301 (2), 726–746.

Garcia-Gonzalez, J., de la Muela, R.M.R., Santos, L.M., Gonzalez, A.M., 2008. Stochastic joint optimization of wind generation and pumped-storage units in an electricity market. IEEE Trans. Power Syst. 23 (2), 460–468.

General Electric, 2019. GE 1.5-77 wind turbine. https://www.ge.com/in/wind-energy/1.5-MW-wind-turbine (Accessed 8 July 2020).

Gomes, I., Melicio, R., Mendes, V., Pousinho, H., 2019. Decision making for sustainable aggregation of clean energy in day-ahead market: Uncertainty and risk. Renew. Energy 133, 692–702.

Gomes, I.L., Pousinho, H., Melicio, R., Mendes, V., 2017. Stochastic coordination of joint wind and photovoltaic systems with energy storage in day-ahead market. Energy 124, 310–320.

Gönsch, J., Hassler, M., 2016. Sell or store? An ADP approach to marketing renewable energy. OR Spectrum 38 (3), 633–660.

Hannah, L., Dunson, D.B., 2011. Approximate dynamic programming for storage problems. In: ICML.

Hassler, M., 2017. Heuristic decision rules for short-term trading of renewable energy with co-located energy storage. Comput. Oper. Res. 83, 199–213.
Hull, J., White, A., 1994. Numerical procedures for implementing term structure models I: Single-factor models. J. Deriv. 2 (1), 7–16.
International Renewable Energy Agency, 2018. Global energy transformation: A roadmap to 2050. https://www.irena.org/-/media/Files/IRENA/Agency/Publication/2018/Apr/IRENA_Report_GET_2018.pdf (Accessed: 24 November 2020).
IRENA, 2021. Electricity storage and renewables: Costs and markets to 2030. https://www.irena.org/-/media/Files/IRENA/Agency/Publication/2017/Oct/IRENA_Electricity_Storage_Costs_2017_Summary.pdf (Accessed 3 May 2022).
Jaillet, P., Ronn, E.I., Tompaidis, S., 2004. Valuation of commodity-based swing options. Manage. Sci. 50, 909–921.
Janczura, J., Trück, S., Weron, R., Wolff, R.C., 2013. Identifying spikes and seasonal components in electricity spot price data: A guide to robust modeling. Energy Econ. 38, 96–110.
Jiang, D.R., Powell, W.B., 2015. Optimal hour-ahead bidding in the real-time electricity market with battery storage using approximate dynamic programming. INFORMS J. Comput. 27 (3), 525–543.
Khazali, A., Rezaei, N., Su, W., Kalantar, M., 2021. Risk-aware bilevel optimal offering strategy of a joint wind/storage unit based on information gap decision theory. IEEE Syst. J. 15 (2), 1939–1949.
Khosravi, M., Afsharnia, S., Farhangi, S., 2022. Stochastic power management strategy for optimal day-ahead scheduling of wind-HESS considering wind power generation and market price uncertainties. Int. J. Electr. Power Energy Syst. 134, 107429.
Kim, J.H., Powell, W.B., 2011. Optimal energy commitments with storage and intermittent supply. Oper. Res. 59 (6), 1347–1360.
Laslett, D., Carter, C., Creagh, C., Jennings, P., 2017. A large-scale renewable electricity supply system by 2030: Solar, wind, energy efficiency, storage and inertia for the South West Interconnected System (SWIS) in Western Australia. Renew. Energy 113, 713–731.
Lew, D., Bird, L., Milligan, M., Speer, B., Wang, X., Carlini, E.M., Estanqueiro, A., Flynn, D., Gomez-Lazaro, E., Menemenlis, N., et al., 2013. Wind and Solar Curtailment. National Renewable Energy Laboratory.
Lisi, F., Edoli, E., 2018. Analyzing and forecasting zonal imbalance signs in the Italian electricity market. Energy J. 39 (5).
Liu, W., Zhang, X., Feng, S., 2019. Does renewable energy policy work? Evidence from a panel data analysis. Renew. Energy 135, 635–642.
Löhndorf, N., Minner, S., 2010. Optimal day-ahead trading and storage of renewable energies—an approximate dynamic programming approach. Energy Syst. 1 (1), 61–77.
Löhndorf, N., Wozabal, D., Minner, S., 2013. Optimizing trading decisions for hydro storage systems using approximate dual dynamic programming. Oper. Res. 61 (4), 810–823.
Lucia, J.J., Schwartz, E.S., 2002. Electricity prices and power derivatives: Evidence from the Nordic Power Exchange. Rev. Deriv. Res. 5 (1), 5–50.
Mathiesen, B.V., Lund, H., Karlsson, K., 2011. 100% Renewable energy systems, climate mitigation and economic growth. Appl. Energy 88 (2), 488–501.
MISO, 2022. Module C - Energy and operating reserve markets. https://docs.misoenergy.org/legalcontent/Module_C_-_Energy_and_Operating_Reserve_Markets.pdf (Accessed 8 June 2022).
Morales, J.M., Conejo, A.J., Madsen, H., Pinson, P., Zugno, M., 2013. Integrating renewables in electricity markets: Operational problems, vol. 205. Springer Science & Business Media.
Nasrolahpour, E., Kazempour, J., Zareipour, H., Rosehart, W.D., 2016. Impacts of ramping inflexibility of conventional generators on strategic operation of energy storage facilities. IEEE Trans. Smart Grid 9 (2), 1334–1344.
NEOEN, 2022. NEOEN gives go ahead on 412 MW wind farm, first stage of its Goyder Renewables Zone in South Australia. https://neoen.com/en/news/2022/neoen-gives-go-ahead-on-412-mw-wind-farm-first-stage-of-its-goyder-renewables-zone-in-south-australia/ (Accessed 8 June 2022).
NOAA, 2019. Integrated surface data, hourly, global. https://www.ncdc.noaa.gov/data-access (Accessed 8 July 2020).
NYISO, 2019. Energy market & operational data. https://www.nyiso.com/energy-market-operational-data (Accessed 8 July 2020).
Papavasiliou, A., Oren, S.S., 2008. Coupling wind generators with deferrable loads. In: 2008 IEEE Energy 2030 Conference. IEEE, pp. 1–7.
Parker, G.G., Tan, B., Kazan, O., 2019. Electric power industry: Operational and public policy challenges and opportunities. Prod. Oper. Manage. 28 (11), 2738–2777.
Peker, M., Kocaman, A.S., Kara, B.Y., 2018. Benefits of transmission switching and energy storage in power systems with high renewable energy penetration. Appl. Energy 228, 1182–1197.
Pina, A., Silva, C.A., Ferrão, P., 2013. High-resolution modeling framework for planning electricity systems with high penetration of renewables. Appl. Energy 112, 215–223.
Pinson, P., Chevallier, C., Kariniotakis, G.N., 2007. Trading wind generation from short-term probabilistic forecasts of wind power. IEEE Trans. Power Syst. 22 (3), 1148–1156.
PJM, 2015. PJM manual 27: Open access transmission tariff accounting. https://www.pjm.com/~/media/documents/manuals/m27.ashx (Accessed 8 June 2022).
Röben, F., De Haan, J.E., 2019. Market response for real-time energy balancing–evidence from three countries. In: 2019 16th International Conference on the European Energy Market. IEEE, pp. 1–5.
Sheskin, T.J., 1985. A Markov chain partitioning algorithm for computing steady state probabilities. Oper. Res. 33 (1), 228–235.
Sunar, N., Birge, J.R., 2019. Strategic commitment to a production schedule with uncertain supply and demand: Renewable energy in day-ahead electricity markets. Manage. Sci. 65 (2), 714–734.
Tauchen, G., 1986. Finite state Markov-chain approximations to univariate and vector autoregressions. Econom. Lett. 20 (2), 177–181.
Terça, G., Wozabal, D., 2020. Economies of scope for electricity storage and variable renewables. IEEE Trans. Power Syst. 36 (2), 1328–1337.
U.S. Department of Energy, 2018. Wind technologies market report. https://www.energy.gov/ (Accessed 12 November 2020).
van der Veen, R.A., Abbasy, A., Hakvoort, R.A., 2012. Agent-based analysis of the impact of the imbalance pricing mechanism on market behavior in electricity balancing markets. Energy Econ. 34 (4), 874–881.
Vilim, M., Botterud, A., 2014. Wind power bidding in electricity markets with high wind penetration. Appl. Energy 118, 141–155.
Wang, Q., Zhang, C., Ding, Y., Xydis, G., Wang, J., Østergaard, J., 2015. Review of real-time electricity markets for integrating distributed energy resources and demand response. Appl. Energy 138, 695–706.
Weitemeyer, S., Kleinhans, D., Vogt, T., Agert, C., 2015. Integration of renewable energy sources in future power systems: The role of storage. Renew. Energy 75, 14–20.
Xu, X., Hu, W., Cao, D., Huang, Q., Liu, Z., Liu, W., Chen, Z., Blaabjerg, F., 2020. Scheduling of wind-battery hybrid system in the electricity market using distributionally robust optimization. Renew. Energy 156, 47–56.
Zhang, Q., Wang, G., Li, Y., Li, H., McLellan, B., Chen, S., 2018. Substitution effect of renewable portfolio standards and renewable energy certificate trading for feed-in tariff. Appl. Energy 227, 426–435.
Zhong, J., Bollen, M., Rönnberg, S., 2021. Towards a 100% renewable energy electricity generation system in Sweden. Renew. Energy 171, 812–824.
Zhou, Y., Scheller-Wolf, A., Secomandi, N., Smith, S., 2019. Managing wind-based electricity generation in the presence of storage and transmission capacity. Prod. Oper. Manage. 28 (4), 970–989.